Background Notes on DICE-2023
Lint Barrage and William Nordhaus
March 22, 2024

The following are background notes that provide supplementary information on the assumptions and modeling for DICE-2023, published in March 2024 in *Proceedings of the National Academy of Sciences (US).* These background notes are the original versions that were submitted with the *PNAS* review and are subject to future revisions.

The study and its online appendix are available at https://yale.app.box.com/s/whlqcr7gtzdm4nxnrfhvap2hlzebuvvm/folder/196571686525.

Table of Contents Page

Background Note on Discounting[1]
Revised December 18, 2023

Advice on Background Note on Discounting: These background notes are for informational purposes for modelers. They are not intended for publication and are not publication quality. Some of the details are sketched and not derived in detail in this document. They may be cited with the warning, "Background notes are for informational purposes and are not published." This note supersedes the previously distributed Note of July 2023.

[1] This background document replaces the earlier one dated October 30, 2023. The approach has been revised to reflect suggestions from several readers, especially William Hogan and Brian Prest. The latter provided valuable advice on the background calculations of the precautionary effect especially in NPP (2022); the underlying simulations and results from NPP have been useful in developing the estimates. We are grateful for suggestions for improvement from Christian Gollier and William Pizer. File is BackgroundNoteOnDiscounting-121823a.docx.

Part A. Summary of approach to discounting

Previous versions of DICE used different approaches to discounting. Upon the advice of modelers and readers, we have revised the treatment to employ an approach known as the "certainty equivalent" rate of return. This approach has been developed using suggestions of William Hogan, theoretical approaches developed by Gollier (particularly 2016), recommendations of the National Academy committee (2017), and empirical implementation of the correction for growth uncertainty by Newell, Pizer, and Prest (2022), hereafter NPP. This summary provides a full discussion of the approach, with other aspects in further Parts of this *Background Note.*

The variables in the analysis are the following. All rates are average annual returns. All time variables are per year.

$R_T =$ discount rate from *0* to T
$r_t =$ discount rate from *t-1* to t
$R_T^f, R_T^K, R_T^{CLIM} =$ risk-free, capital, and climate discount rates
$\rho =$ pure rate of time preference
$\varphi =$ elasticity of utility with respect to consumption
$\rho_T^* =$ risk-adjusted rate of time preference
$g_T =$ average growth of per capita consumption from *0* to T
$P_T =$ precautionary effect rate from *0* to T
$\sigma_C^2 =$ variance of trend growth rate of per capita consumption
$\pi =$ capital premium
$\beta^{CLIM} =$ climate beta
$\tilde{x}_T =$ deterministic version of variable x_T

As in earlier versions of the DICE model, discounting continues to follow the approach of the Ramsey-Cass-Koopmans growth model in determining real rates of return. In this approach, the continuous-time equilibrium deterministic long-run rate of return from 0 to T $\left(\tilde{R}_T\right)$ is given by the pure rate of time preference *(ρ)* plus the product of the deterministic growth rate of per capita consumption from t = 0 to T $\left(\tilde{g}_T\right)$ times the elasticity of the marginal

utility of consumption *(φ)*. Note that the "~" over a variable indicates a deterministic concept.

$$(\text{A.1}) \quad \tilde{R}_T = \rho + \varphi \tilde{g}_T$$

In many applications, the consumption elasticity *(φ)* is also assumed to equal the relative rate of risk aversion. This is *not* assumed in the DICE treatment of discounting. That assumption would lead to a capital risk premium that is far below the observed rate, as is discussed in the literature on the equity-premium puzzle. Instead, we rely on the CAPM estimates of the capital premium.

Our implementation of the modeling continues to rely on the Ramsey model. However, we interpret the elasticity of consumption *(φ)* as applying to relative valuations of consumption over time or the rate of inequality aversion (RIA) but not, as is often commonly assumed, to the relative rate of risk aversion (RRRA). For clarity, we label this the "Ramsey growth model."

Often, IAMs employ the "Ramsey/C-CAPM" approach in which the elasticity of consumption *(φ)* represents both the RIA and the RRRA. This is the approach of NPP and Rennert et al. (2022), for example. The Ramsey/C-CAPM approach is theoretically appealing because it unifies choice over time and over uncertain states of the world. However, that approach fails to generate a realistic risk premium (hence, the equity premium puzzle), and for this reason is not used in DICE-2023. Other extensions, such as the Epstein-Zin specification, introduce different RIA and RRRA, but these do not solve the equity premium puzzle without raising new complications. (This topic is discussed in detail below in this section and in Part E.)

As we use the term, the Ramsey growth model does not include any risk aversion in deriving what is called "the precautionary effect." Rather, alternative growth paths generate alternative discount rates (as per Weitzman, 1998). While we use the terminology of the precautionary effect, the interpretation is that it is an adjustment for uncertain growth and for inequality aversion. While we could add a separate approach to account for risk aversion, we have found no satisfactory unified model and choose to take the simpler CAPM approach, which is not rigorously connected to the Ramsey growth model but has a firm empirical foundation.

The modeling relies upon discount rates and their associated discount factors to calculate present values, optimal policies, and variables such as the social cost of carbon. The "discount factor," D_T, is the factor applied to future values to obtain the present value of a value in time *T* discounted back to time *0*. In a deterministic framework, the discount factor is the product of the one-period discount factors. In this discussion, r_t are period-to-period rates of return from period *(t-1)* to *t*, while R_T are long rates of return from period *0* to period *T* (all in compound annual rates).

$$(A.2) \quad D_T = \left[\frac{1}{\left(1+R_T\right)^T}\right] = \left[\frac{1}{\left(1+r_1\right)}\right]\left[\frac{1}{\left(1+r_2\right)}\right]\ldots\left[\frac{1}{\left(1+r_T\right)}\right]$$

Because of uncertainty about future growth, the *expected* discount factor will differ from the deterministic discount factor by a term called the "precautionary effect." For example, with two interest rate paths which differ by a constant 4% per year for 100 years, the precautionary effect is to lower the average 100-year long rate by 1.3% points. The effect on the near term is small, with a precautionary effect of only 0.04%/year in the second period (2025). However, with long horizons, the impact of uncertain growth can be substantial, and for that reason the precautionary effect has a major impact on climate policy.

In the approach taken here, we assume that the major uncertainty is about the long-run *trend* rate of growth of per capita consumption. More precisely, we assume that the trend rate of growth of per capita consumption is normally distributed with a constant variance of $\sigma_C{}^2$.. Note that the variance of log consumption will grow as $\sigma_C{}^2 T^2$, which is different from the usual model of the equity premium where the variance of log consumption is constant over time. The next section shows a numerical example to show the impact of random trend growth.

The precautionary component for this distribution of trend growth rates is given by

$$(A.3) \quad P_T = -\tfrac{1}{2}\,\sigma_C{}^2 \varphi^2 T$$

where P_T = is the precautionary effect from time *0* to *T* and $\sigma_C{}^2$ is the variance of the trend growth rate of consumption. In a process where there is uncertainty about the trend rate of growth, the precautionary effect will be larger as the length of period increases because the variance of log consumption increases. For a deterministic model like DICE, we therefore correct the deterministic Ramsey equation to reflect growth uncertainty through adding the precautionary effect.

This procedure generates a sequence of "certainty-equivalent discount rates." This term is used to designate the single discount rate delivering the same discount factor as the expected value from the distribution of uncertain future discount rates (NPP, p. 1019). From (A.1) and (A.3), the certainty-equivalent risk-free discount rates $\left(R_T^f\right)$ are given by (A.4):[2]

$$(\text{A.4}) \quad R_T^f = \rho + \varphi\, \tilde{g}_T - \tfrac{1}{2}\, \sigma_C{}^2 \varphi^2 T$$

To calculate the precautionary effect, we examine two procedures. The first is based on the calculations of NPP. These take estimated future growth rates from their Monte Carlo draws and the implied future interest-rate structure to estimate numerically the precautionary component. A second approach takes the standard formula in (A.3) for the precautionary effect from a model with a normal distribution of trend growth rates. The two approaches give reasonably similar estimates of the precautionary effect, and we therefore take equation (A.3) as computationally simpler and easier to implement and test. For a comparison of the two approaches, see the derivation of the precautionary effect in Part D.

The key parameters of the precautionary effect are the variance of the consumption growth rate and the consumption elasticity. The variance is estimated in several studies (e.g., Christensen. Gillingham, and Nordhaus 2018 and Müller, Stock, and Watson 2022). The studies have estimates of the standard deviation of trend per capita consumption growth to 2100 in the range of 1.0% to 1.2% per year. For our modeling, we assume that trend growth of consumption per capita follows a normal distribution with a mean of

[2] See, e.g., Prest (2023) equation (1) or Gollier (2016) equation (37), where we note in reference to the latter that our approach to discounting uses the CAPM rather than CCAPM approach for adjustments to the risk profile of climate investments, as discussed below.

2% per year and standard deviation of 1 percentage point per year. Part D describes the calculation of the precautionary effect in detail. Part F provides updated estimates of future economic growth.

In making calculations for DICE-2023, we rely on two components of the discount rate: a risk-free rate and an adjustment for investment risk. A broad consensus exists that the risk-free real return on investment is in the range of 0 to 2% per year over the last century. We take 2% per year to be the rate for long-term risk-free investments, which is the rate that has prevailed over the last century or so except for the most recent period.

Empirical evidence indicates that the return to risky assets (such as corporate capital or an unleveraged portfolio of corporate equities) is substantially higher than the risk-free rate. For example, the post-tax average rate of return on US corporate capital has averaged around 7% per year over the period from 1948 to 2022. The real return on a deleveraged portfolio of large US public corporations was 6% per year for the same period. The underlying data are presented in Part E.

At this point, we confront the "equity premium puzzle." This puzzle is that the volatility of consumption cannot rationalize the high risk premium (of 5% per year in our estimates) within the standard model (the C-CAPM model). Most studies examine the equity premium, but the puzzle remains for capital as well as equity. Given the failure of the C-CAPM model, we adopt the estimates from the CAPM model, which examines the correlation of investment risks with the market risk rather than the consumption risk. This leads to the assumption of a risk premium of 5% per year in the DICE-2023 model. Note that our approach differs from those that take the C-CAPM approach (such as Gollier 2014 and NPP).

In the new DICE-2023 specification, the discount rate includes an adjustment for the non-diversifiable risk of climate investments. Risky climate investments, primarily those to reduce emissions and reduce future damages, are introduced through the concept of the climate beta. The climate beta measures the extent to which climate investments (such as renewable power) share the non-diversifiable risk characteristics of the economy's aggregate investments. A climate beta of zero indicates that the risks on climate investments are uncorrelated with market returns; a climate beta of one indicates that climate investments have risk properties similar to those of the aggregate economy. We take our estimate of the climate beta from Dietz et al.

(2020), which estimates a long-run climate beta of 0.5, so one with an intermediate correlation with market risks. A more extensive discussion of the climate beta and the reason for our estimate is given in Part C.

For our purposes, we assume that the near-term risk-free long-term rate is 2% per year and the capital risk premium is π = 5% per year. With a climate beta of 0.5, this implies a near-term risk-adjusted certainty-equivalent discount rate on climate investments of 2% + 0.5 x 5% = 4.5% per year. We note that the precautionary adjustment is taken to be zero in this illustrative calculation as near-term consumption growth trend uncertainty is minimal.

To calibrate the model requires estimates of φ and ρ. These are estimated by first calculating the deterministic risk-free rate of return from (A-1) above (where we note that using the certainty-equivalent rate equation (A-4) would yield equivalent results again due to the small level of near-term growth uncertainty). We constrain ρ ≥ 0.1% per year to ensure long-run convergence and for consistency with the estimates in NPP; we then incorporate the DICE estimates of near-term growth in per capita consumption of 2% per year. These parameters lead to the bound that ρ = 0.1% per year. Solving for φ gives the following:

$$(A.5) \quad \varphi = \frac{\left(R^{f}_{2020} - \rho\right)}{g_{2020}} = \frac{(0.02 - 0.001)}{0.02} = 0.95$$

This then implies that the average annual discount rate on climate investments (R_T^{CLIM}) from *0* to *T* is:

$$(A.6) \quad R_T^{CLIM} = \rho + \varphi \tilde{g}_T - \tfrac{1}{2}\varphi^2 {\sigma_C}^2 T + \beta^{CLIM}\pi$$

With an estimated climate beta of 0.5 as well as other estimates, this leads to a near-term *(T = 0)* rate of return on climate investments of 4.5% per year.

$$(A.7) \quad \begin{aligned} R_0^{CLIM} &= 0.001 + (0.95)(0.02) - \tfrac{1}{2}(0.95)^2(.01)^2(0) + (0.5)(0.05) \\ &= 0.045 \end{aligned}$$

This calculation gives an estimate of 4.5% per year for the near term.

In order to implement (A.6) in DICE, we replace the pure rate of social time preference in equation (A.1) with a "risk-adjusted rate of time preference" designated by $\rho_T^* = \rho - \tfrac{1}{2}\varphi^2 {\sigma_C}^2 T + \beta^{CLIM}\pi$.

Growth v level precautionary effect: An example

For those used to the standard equity-premium model, the precautionary calculation used here may be unfamiliar. In the standard model (such as Mehra and Prescott 1985), the growth of log consumption is an i.i.d. random variable. We can illustrate the difference between the level effect and the growth effect on the precautionary term with a simple example. For this example, we assume that the consumption elasticity is $\varphi = 1$. In the *level effect,* we assume that growth of log consumption has a zero trend with i.i.d. random normal disturbances over time with a standard deviation of $\sigma_{C,L} = 0.02$. The precautionary effect in this case is $P_T = -½\ {\sigma_{C,L}}^2 \varphi^2 = -½ * 0.0004 * 1 = -0.0002$, which is constant over time.

With the *growth effect*, we assume that the trend rate of growth has a normal distribution with a zero mean and a standard deviation of $\sigma_{C,g} = 0.01$ per year. In the growth case, the precautionary effect is

$$P_T = -½\ {\sigma_{C,g}}^2 \varphi^2 T = -½ * (0.0001) * 1 * T = -0.00005 * T.$$

Thus, while the level precautionary effect is constant at -0.02%/year, the growth precautionary effect starts out at -0.005%/year in year T = 1 and increases to -1.5%/year after 300 years. The reason is that the variance of log consumption across paths is constant with the level effect and increases with time with the growth effect.

Figure A-1 shows six paths, which are displayed on a logarithmic vertical scale. The three paths that are closely packed in the middle are the three randomly chosen paths with only the level effect. The three dispersed paths are three paths with randomly selected constant growth rates. As is clear from this example, the standard deviation of the growth paths is linear in time, while the standard deviation of the level paths is roughly constant over time.

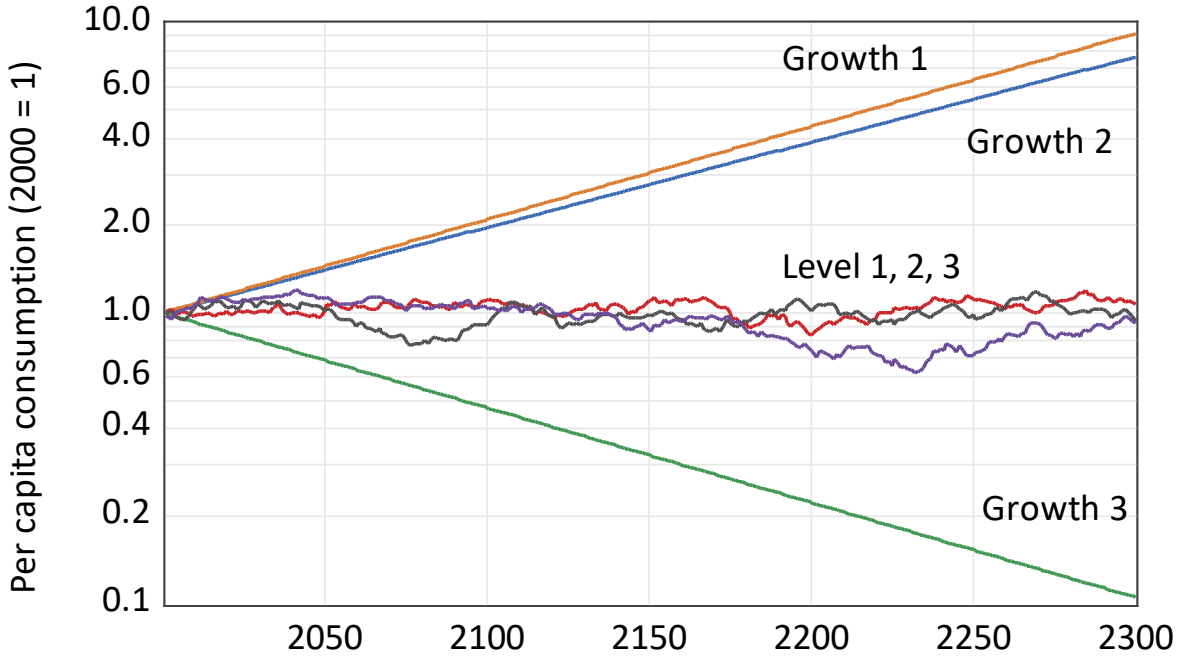

Figure A-1. Figure shows per capita consumption with randomly selected paths. These show three paths with random level effects and three paths with random growth effects. Note that the three growth paths diverge over time and have a standard deviation that is approximately linear in time. This indicates why the precautionary effect is linear in time in DICE under the assumption of random trend growth rates.

Part B. **GAMS programming for discounting**

The following is the GAMS programming code in DICE-2023 that determines discounting (file is "DICE2023-b-4-3-10.gms").

```
PARAMETERS
[other]
** Preferences, growth uncertainty, and timing
        betaclim  Climate beta                                      / 0.5  /
        elasmu    Elasticity of marginal utility of consumption     / 0.95 /
        prstp     Pure rate of social time preference               /.001/
        pi        Capital risk premium                              / .05  /
        rartp       Risk-adjusted rate of time preference
        k0        Initial capital stock calibrated (1012 2019 USD)  / 295  /
        siggc1    Annual standard deviation of consumption growth   / .01 /
** Scaling so that MU(C(1)) = 1 and objective function = PV consumption
        tstep       Years per Period                                / 5  /
        SRF         Scaling factor discounting                      /1000000/
[other]
PARAMETERS
[other]
** Precautionary dynamic parameters
        varpcc(t)         Variance of per capita consumption
        rprecaut(t)       Precautionary rate of return
        RR(t)             STP with precautionary factor
        RR1(t)            STP factor without precautionary factor;
** Time preference for climate investments and precautionary effect
        rartp           = exp( prstp + betaclim*pi)-1;
        varpcc(t)       =  min(Siggc1**2*5*(t.val-1),Siggc1**2*5*47);
        rprecaut(t)     = -0.5*varpcc(t)*elasmu**2;
        RR1(t)          = 1/((1+rartp)**(tstep*(t.val-1)));
        RR(t)           = RR1(t)*(1+rprecaut(t))**(-tstep*(t.val-1));
[other]
VARIABLES
[other]
        TOTPERIODU(t)   Period utility
        UTILITY         Welfare function
        RFACTLONG(t)
        RSHORT(t)       Real interest rate with precautionary(per annum year on year)
        RLONG(t)        Real interest rate from year 0 to T
;
[other]
*Economic variables
        RSHORTEQ(t)      Short-run interest rate equation
        RLONGeq(t)       Long-run interest rate equation
        RFACTLONGeq(t)   Long interest factor
* Utility
        TOTPERIODUEQ(t)  Period utility
        PERIODUEQ(t)     Instantaneous utility function equation
        UTILEQ           Objective function      ;

[other]
**** Equations of the model
[other]
**Economic variables
 RFACTLONGeq(t+1)..   RFACTLONG(t+1) =E= SRF*(cpc(t+1)/cpc('1'))**(-elasmu)*rr(t+1);
 RLONGeq(t+1)..       RLONG(t+1)     =E= -log(RFACTLONG(t+1)/SRF)/(5*t.val);
 RSHORTeq(t+1)..      RSHORT(t+1)    =E= -log(RFACTLONG(t+1)/Rfactlong(t))/5;
** Welfare functions
 periodueq(t)..       PERIODU(t)     =E= ((C(T)*1000/L(T))**(1-elasmu)-1)/(1-elasmu)-1;
 totperiodueq(t)..    TOTPERIODU(t)  =E= PERIODU(t) * L(t) * RR(t);
 utileq..             UTILITY        =E= tstep * scale1 * sum(t,  TOTPERIODU(t)) + scale2;
```

Part C. **Calculation of the climate beta**

Estimates of the climate beta are scarce. The most comprehensive estimate is from Dietz et al. (2018), which uses a combination of theory and integrated assessment modelling (IAM) to estimate the climate beta. While their IAM empirical estimates rely on an earlier version of DICE, the study uses parametric uncertainties for the DICE model and adds further potential parametric uncertainties, such as those for catastrophic damages. Their long-run estimate (to 2215) for all uncertainties is beta = 0.49 (see their Table 3). However, depending upon the combination of uncertainties, the estimates range as high as 1.10. The surprisingly high beta is driven largely by the dominance of the uncertainty about TFP growth, which they assume to be normal with a standard deviation of 0.9% per year. This estimate is close to the estimate we use (1% per year) for determining the precautionary effect in DICE-2023.

Note that from an analytical point of view, as they show, the climate beta is likely to be at least 1 if the uncertainties are driven largely by uncertainty of the growth of productivity (and therefore per capita consumption). The surprising result is, as Dietz et al. clearly explain, "the positive effect on the climate beta of uncertainty about exogenous, emissions-neutral technological progress overwhelms the negative effect on the climate beta of uncertainty about the carbon-climate-response, particularly the climate sensitivity, and the damage intensity of warming." (p. 258)

A different approach to estimating the climate beta comes from estimates of industry betas for sectors where the major mitigation investments are likely to be made. For example, replacing electricity generated by fossil fuel will require generation by renewables. If we take power, utilities, and air transport as three highly carbon-intensive industries, we can examine estimates of CAPM betas from Professor Aswath Damodaran (https://pages.stern.nyu.edu/~adamodar/). For these three industries, the average unleveraged betas are calculated to be 0.49, which is reasonably close to the estimates we use from Dietz et al.

We conclude that we assume a climate beta of 0.5 for the present version of DICE-2023. However, we emphasize that this estimate contains considerable uncertainty both in terms of its empirical basis (since it is model-based rather than historically-based) and also that the estimate is strictly speaking appropriate for the C-CAPM framework where it was derived.

Part D. **Estimates of the precautionary effect**

For long-term projections, it is important to include the impacts of the uncertainty about future economic growth on discounting, a factor that has been ignored in earlier vintages of the DICE model. This note uses the approach of Newell, Pizer, and Prest, "NPP" (2022) to estimate the impact of growth uncertainty. We call this higher-order impact "the precautionary term." Note, however, as discussed in the introduction to this Note, that this term is widely used but in the present context refers to the impact of growth uncertainty on discounting that operates through the intertemporal elasticity, not risk aversion.

The basic analysis is well known but is usefully described in Gollier (2016). In the standard Ramsey model where P_T is the precautionary effect from t = 0 to T, φ is the intertemporal consumption elasticity, and the trend consumption growth rate follows a normal distribution with a variance of σ_c^2, the precautionary effect is given by:

$$(D.1) \quad P_T = -½\varphi^2\sigma_c^2 T$$

The precautionary effect is introduced as an exogenous variable since there is no uncertainty in the DICE model. This term is calculated using estimates of the uncertainty of trend growth of per capita consumption along with assumptions about the key parameter of φ. There are several estimates of the long-run path of growth uncertainty, but they are all reasonably consistent.

Monte Carlo with lognormal output

The simplest approach uses a Monte Carlo simulation. For this simulation, we assume that trend growth in consumption is distributed as $\mathcal{N}$(mean growth, standard deviation of trend growth) = $\mathcal{N}$(0.02, 0.01), ρ = .001, φ = .95, and N = 10,000 replications. To be clear, draw one might have constant consumption growth rates of 1.6% per year, draw 2 perhaps 2.5% per year, and so forth. Table D-1 shows the results for long-run real returns. The parametric assumptions are in the legend of the table. Here are the key points:

- The deterministic risk-free discount rate is a constant 2% per year. This reflects the constant expected rate of growth of output with the assumed values of ρ and φ.
- The certainty-equivalent discount rate is lower than the deterministic rate by the precautionary rate. At 80 years (2100 in the model), with the empirical assumptions above, the certainty-equivalent discount rate would be 36 basis points lower than the

deterministic rate as defined here and more generally in the literature. By 280 years (2300), the precautionary effect is 121 basis points. Because of the assumptions, the precautionary rate is linear in time.

- The numerical calculation using the Monte Carlo is virtually identical to the formulaic calculation of the precautionary effect.

Period from present	R^{CE}	R^{DETER}	$R^{PRECAUT}$	$R^{PRECAUT}$calc	$R^{PRECAUT}$ minus RP^{RECAUT}calc	Sample	sigma(g)	ρ	φ
1	1.99%	2.00%	0.004%	0.005%	0.000%	10,000	0.01	0.001	0.95
30	1.86%	2.00%	0.134%	0.135%	-0.001%	10,000	0.01	0.001	0.95
80	1.64%	2.00%	0.358%	0.361%	-0.003%	10,000	0.01	0.001	0.95
180	1.20%	2.00%	0.798%	0.812%	-0.014%	10,000	0.01	0.001	0.95
280	0.78%	2.00%	1.215%	1.264%	-0.048%	10,000	0.01	0.001	0.95

ρ =	0.1%
φ =	0.95
N =	10,000
g (p.c. cons)=	N(.02, .01)
R^{CE} =	Certainty equivalent discount rate
R^{DETER} =	Deterministic rate (rate implied by average growth rate)
$R^{PRECAUT}$ =	Precautionary component determined by concavity ($-\frac{1}{2}\varphi^2\sigma_T^2$)
$R^{PRECAUT}$_CALC =	Precautionary component determined by lognormal formula ($-\frac{1}{2}\varphi^2(\sigma_{C,T})^2$)

Table D-1. Estimates of the precautionary effect using a normal distribution for trend growth of consumption[i].

Note that φ in the Table refers to the consumption elasticity.

NPP Estimates

A second approach uses the growth estimates from NPP (2022). For these, we use the results of the NPP Monte Carlo of consumption growth based on Muller et al. (2022) provided by the authors to calculate the precautionary effect.[ii] Note that these estimates differ in the levels from Christensen et al. (2018) or Rennert et al. (2022) but the variance is reasonably close. These use the same parameters as the first approach, but in NPP there is a random

element to the level of consumption along with a slightly changing variance in the trend growth rate.

Figure D-1 shows the variance over time of the analytical approach above ("DICE variance") along with the variance determined by the NPP draws. The NPP has a higher short run variance because of the random element in the level of consumption, while the trend is slightly lower in NPP, with a cross-over at about 120 years. Note as well that the DICE variance is linear by assumption.[iii] Since the difference between the two precautionary effect is close to half of the difference between the two variance estimates, the precautionary effect with be close to 10 basis points higher for the NPP estimates in the first 50 years, then approximately the same for the next century or so, then lower after about 200 years.

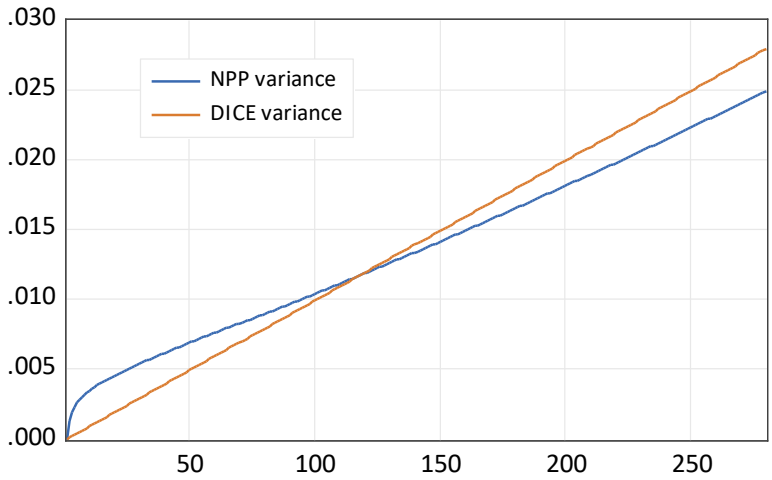

Figure D-1. Comparison of the variance of the growth rate of consumption under the two approaches.

Part E. **Historical rates of return**

We have gathered in Table E-1 data on total returns for major assets classes in the US for the 1927- 2022 period with thanks to the Stern School. Note that these are total returns including dividends, interest, and capital gains or losses.

Additionally, Table E-2 provides estimates of the rate of return (total earnings on capital, i.e., profits plus interest) as a percentage of the current replacement cost of the net stock of fixed assets of the US corporate sector based on data from the US BEA.

Year	*S&P 500*	*3-month T.Bill*	*US T. Bond*	*Baa Bond*	*Real Estate*
Arithmetic Average Historical Return					
1928-2022	11.5%	3.3%	4.9%	7.0%	4.4%
1973-2022	11.7%	4.4%	6.6%	8.8%	5.5%
2013-2022	13.6%	0.8%	0.5%	3.8%	7.7%
Arithmetic Average Real Return					
1928-2022	8.3%	0.3%	1.9%	3.9%	1.3%
1973-2022	7.6%	0.4%	2.6%	4.7%	1.5%
2013-2022	10.8%	-1.8%	-1.9%	1.3%	4.9%

Table E- 1. Total returns on US financial assets

Source: Data from NYU, Stern School, https://pages.stern.nyu.edu/~adamodar/New_Home_Page/datafile/histretSP.html in file "stern-returns-2023.xlsx"

[Real returns are not available as geometric averages from the source.]

	Return before taxes (all corps)	Return after taxes (all corps)	Return before taxes (non-fin corps)	Return after taxes (non-fin corps)
1948 - 2022	11.0%	7.6%		
1992 - 2022	10.6%	8.6%		
1998 - 2017	10.2%	7.9%	8.8%	7.2%
2012 - 2022	11.1%	9.3%		

Table E- 2. Rates of returns on capital of US corporations

Rates of return are total capital income divided by replacement cost of capital, both in current prices. They are conceptually real returns. Data from the BEA. These include S corporations. A correction for the share of S corporations reduces the return over the last two decades by about 50 basis points.[iv]

Based on these findings, we conclude the following:

1. The *short-run* risk-free return (measured as the real return on short Treasury securities) has averaged close to zero per year for most of the last century, although it has been lower in recent years.
2. The *long-run* risk-free rate of return (measured on 10-year Treasury bonds) has averaged around 2% per year over the total period, although it has been sharply lower in the last decade. The real interest rate on 10-year TIPS has a shorter period and has recently risen back to the earlier pre-financial crisis level of about 2% per year real.
3. The best estimate of the after-tax real return on capital (measured in the US corporate sector) has been 7 – 9% per year over the last half-century. Unlike financial returns there has been no major change in these returns in the last two decades.
4. Corporate equities are currently unleveraged with respect to total bond-type assets. The aggregate US corporate non-financial balance sheet has a long-debt/equity ratio of approximately 30% with a roughly equal short-debt/equity ratio. We therefore treat corporate equities as unleveraged.

The capital premium

We define the "capital premium" as the difference between the expected return on aggregate economy-wide assets and the risk-free rate of return. Based on the current balance sheet of the corporate sector, we assume that the capital premium is the same as the well-studied equity premium.[3] We observe these data only for the US non-financial corporate sector and assume that these values apply to the entire global financial structure. Based on the estimates above, we assume that the rate of return on risky assets in the US is 7% per year and has been relatively stable. That rate applies not only to financial returns but also to corporate capital. Based on the estimate of a risk-free long-run rate of return of 2% per year, we calculate the capital premium to be 5% per year.

We note at this point the difficulty of estimating various rates of return given the volatility of the series and the limited sample size. As an example, we can calculate the capital premium as the difference between the risky rate of return on corporate equities and the risk-free return. For 1928 – 2022, the geometric average capital premium is 5.7% per year, with a standard deviation of 2.0% per year. If we assume that the capital premium is i. i. d. normal, then the (5, 95) %ile for the mean return is (3.7%, 7.7%) per year. While this range is well above zero and above the estimates of the equity or capital premium from C-CAPM models, it is clear that there is considerable uncertainty about the estimate of the capital premium.

[3] The literature generally deals with the "equity premium puzzle," dating back to 1985 with Rajnish Mehra, and Edward C. Prescott (1985) and Rajnish Mehra (2008). We use the term capital rather than equity to emphasize that it applies to the return on capital more generally as is appropriate for Ramsey-type models.

Part F. **Revised estimates of economic growth**

Projections of future growth of per capita output and consumption have been revised in October 2023 in light of recent data and research. The results relative to earlier models and versions yield a slightly lower growth rate in the early years (to 2050), but more rapid growth in per capita global output over the model horizon. Note that the growth rates after 2150 make little difference in scenarios with strong policies, but they can affect the base (current policy). The reason is that most strong policies have virtually 100% emissions control after a century, so growth projections after that will have little to no effect on emissions, concentrations, and temperature.

Historical data and current projections are shown in Table F-1. The DICE-2023 projections in the last column are intermediate between the CGN/MSW results and the Rennert et al. (2022) blended statistical and expert elicitations. Figure F-1 visualizes the comparison between DICE-2023, Rennert et al. ("RFF-SPs"), and the NPP projections along with their respective 5-95th percentile ranges.

	Historical data (geometric mean, percent per year)						
	MSW	IMF	CGN	MSW	Renn-med	Renn-avg	DICE-2023
1901-1931	1.3						
1931 - 1960	1.9						
1961 - 1990	2.1	2.3					
1991 - 2022		2.0					
	Projections (geometric mean, percent per year)						
2020 - 2050			2.6	1.9	1.5	1.5	1.9
2020 - 2100			2.0	1.9	1.5	1.5	1.8
2020 - 2200				1.9	0.9	1.1	1.7
2020 - 2300				1.9	0.9	1.1	1.6

MSW = Muller, Stock, and Watson
IMF = International Monetary Fund from historical data base
CGN = Christensen, Gillingham, and Nordhaus
MSW = Muller, Stock, and Watson
Renn-med= Rennert et al., Figure 6 (from background data)
Renn-avg = Rennert et al., Figure 6 (from our calculations)
DICE-2023 = from base run of version b-4-3-6

Table F-1. Estimates of the growth in per capita output from different studies.[v]

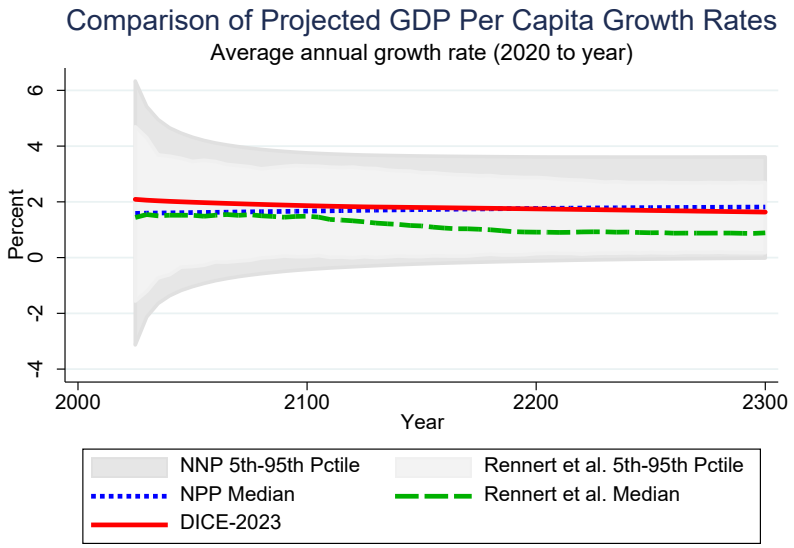

Figure F-1: Comparison of DICE-2023 GDP per capita growth projections with NPP and Rennert et al. medians and 5-95th percentile ranges. Growth is measured as annual average percent growth from 2020 through each depicted year.

A key parameter for calculating the precautionary effect on discounting is the uncertainty about future growth. For this parameter, we examined the dispersion of forecasts. Standard deviations or quantiles of the distributions of growth rates were tabulated in different studies, and these yielded the estimated standard deviations of trend growth in per capita global output shown in Table F-2.

	Estimated standard deviation of trend growth (% points/year)				
	CGN	MSW	NPP	Renn	DICE-2023
2020 - 2050	1.1	1.0	1.0	0.9	1.0
2020 - 2100	1.1	1.0	0.8	0.8	1.0
2020 - 2200			0.8	0.7	1.0
2020 - 2300			0.9	0.6	1.0

CGN = Christensen, Gillingham, and Nordhaus
MSW = Muller, Stock, and Watson
NPP = Newell, Pizer, Prest
Renn = Rennert et al., Figure 6, calculated from (5,95) percentiles.
DICE-2023 = from base run of version b-4-3-6

Table F-2. Estimates of the uncertainty of the growth in per capita output from different studies. [vi]

The estimated standard deviation of the growth rate from 2020 to 2100 ranges from 0.8% to 1.1% points per year. The standard deviation for longer periods ranges between 0.6% to 0.9% points per year depending on period and study. These are significantly larger than the historical variability in growth rates, such as the difference in long-period growth rates in MSW of around 0.4% point per year or estimates of the 1950 – 2022 standard deviation of the growth rate of 0.3% - 0.5% point per year.

For our estimates, we have chosen the estimates from GGN, NPP, and MSW because of our preference for statistical techniques in deriving variability estimates. The main effect of the higher estimate of the uncertainty in the trend growth rate will be to increase the precautionary effect and thereby to lower long-run discount rates, primarily after 2100. For modeling purposes, we choose a constant uncertainty of 1.0% point per year because of the simplicity of modeling and transparency of interpretation. This rate is close to the near-term uncertainty for most estimates but lower than estimates after 2100. Since the precautionary impact is proportional to the variance times the squared time-from-present, this assumption will tend to overestimate the precautionary impact after 2100.

Background

Table F-3 shows the estimates from Christensen et al. (2018). The estimates that are used are the expert results for the world.

Table 1. Expert and low-frequency estimates by region and time horizon

		2010–2050							2010–2100						
Region	Statistic	10th	25th	50th	75th	90th	μ	σ	10th	25th	50th	75th	90th	μ	σ
World	Expert TM	1.17	1.80	2.59	3.23	3.92	2.54	1.07	0.60	1.36	2.03	2.85	3.47	2.06	1.12
	Expert (SD)	1.37	0.97	0.75	0.85	0.92	—	—	2.14	1.14	0.84	0.94	1.06	—	—
	Low freq	1.2	1.7	2.2	2.7	3.3	2.23	0.99	1.2	1.7	2.2	2.7	3.3	2.23	0.98
High	Expert TM	0.56	1.23	1.76	2.30	2.75	1.72	0.84	0.27	0.95	1.46	2.08	2.57	1.47	0.88
	Expert (SD)	1.38	0.82	0.68	0.69	0.77	—	—	1.55	0.92	0.62	0.73	0.84	—	—
	Low freq	0.7	1.4	2.0	2.5	3.0	1.90	0.99	1.0	1.5	2.0	2.4	2.8	1.92	0.89
Middle	Expert TM	0.93	1.76	2.67	3.36	4.11	2.57	1.23	0.34	1.30	1.98	2.72	3.45	1.96	1.18
	Expert (SD)	1.47	0.91	0.77	0.68	0.77	—	—	2.15	0.83	0.81	0.64	0.97	—	—
	Low freq	0.5	1.2	1.9	2.6	3.4	1.92	1.27	0.5	1.3	1.9	2.6	3.4	1.94	1.41
Low	Expert TM	1.05	2.23	3.41	4.25	5.12	3.21	1.57	0.62	1.72	2.53	3.45	4.57	2.58	1.49
	Expert (SD)	1.70	1.25	0.78	0.95	1.26	—	—	2.10	1.23	1.10	1.05	1.55	—	—
	Low freq	2.8	4.3	6.1	8.1	10.2	6.34	3.00	1.8	3.5	5.5	7.9	10.7	5.95	3.74
United States	Expert TM	0.60	1.14	1.75	2.18	2.63	1.66	0.79	0.49	0.91	1.53	2.04	2.64	1.52	0.84
	Expert (SD)	1.18	0.76	0.75	0.69	0.68	—	—	1.28	0.76	0.76	0.65	0.78	—	—
	Low freq	0.9	1.5	2.2	2.8	3.4	2.14	1.09	1.2	1.7	2.1	2.5	2.9	2.03	0.84
China	Expert TM	1.51	2.81	4.23	5.19	6.31	4.01	1.85	0.89	2.02	2.93	3.87	4.87	2.92	1.51
	Expert (SD)	1.83	1.57	1.11	1.18	1.35	—	—	2.29	1.59	1.25	1.15	1.38	—	—
	Low freq	1.6	3.9	6.6	9.5	12.7	6.93	4.61	0.7	3.1	5.7	8.9	12.7	6.33	5.36

Note: Expert and low-frequency estimates by region and time horizon. Expert TM and SD are the trimmed mean and SD of expert forecasts at each quantile. Low-frequency forecasts are Bayes estimates at each quantile. Notation is that μ and σ are the means and SDs of the respective forecast distributions. Expert μ and σ are estimated using a fitted normal distribution (see *SI Appendix* for details).

Table F-3. Projections from Christensen et al. (2018).

Simulations by NPP using Muller et al. (2022) produce the results in Figure F-1 for the distribution of per capita growth, slightly below 2% per year.:

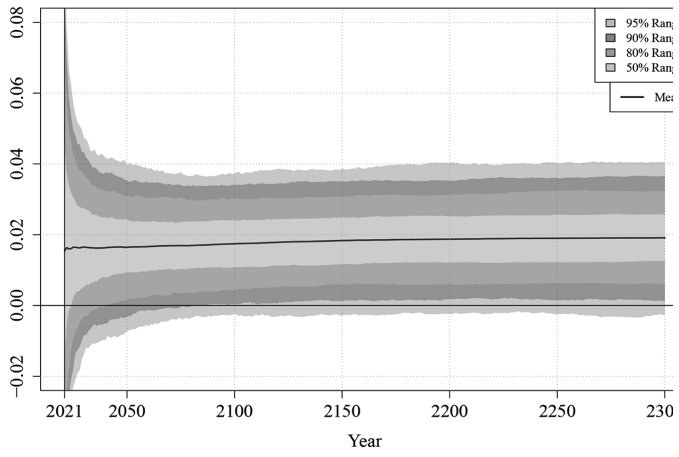

Figure F-1. Distribution of projections of per capita output from NPP

We can compare this to Rennert et al. (2022). The estimates use the "RFF-SPs" to calculate both the median and the uncertainty of future growth rates. These are shown in Figure F-2. Table F-4 shows estimates of the growth rate from Muller et al.

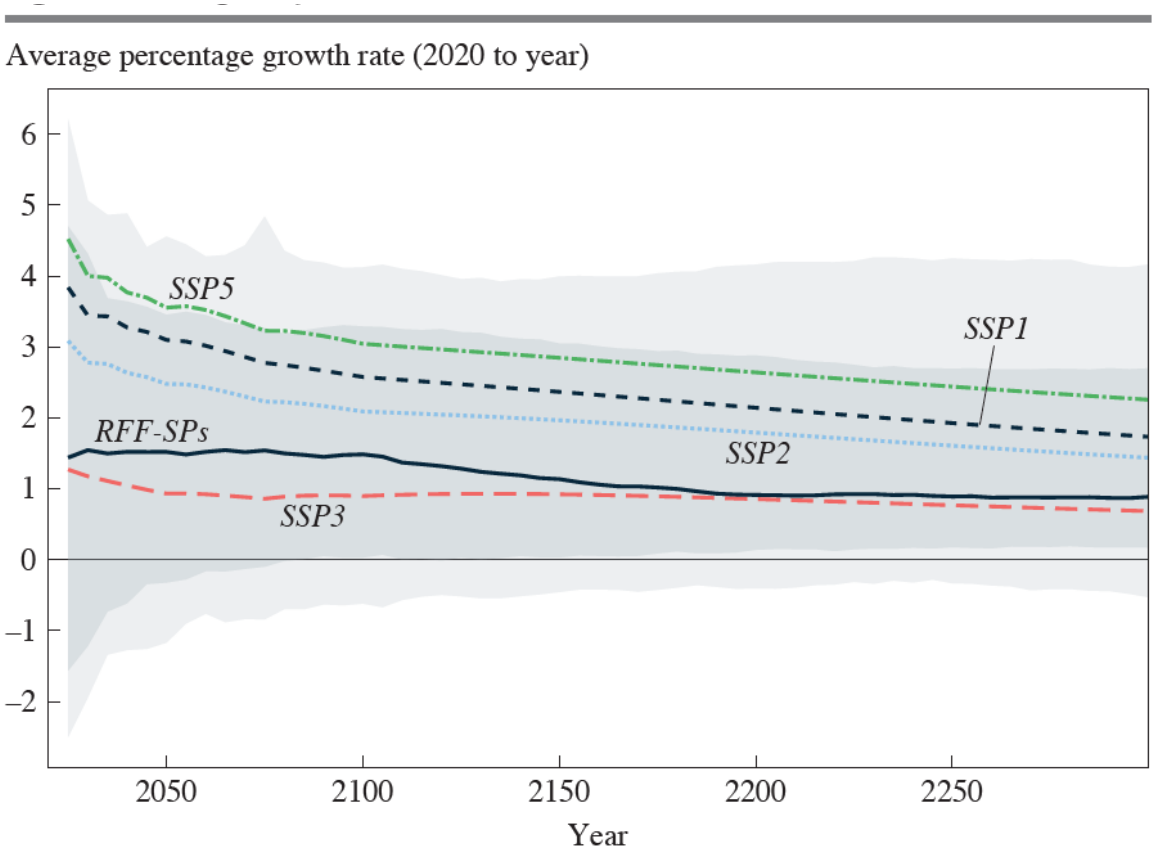

Figure F-2. Distribution of projections of per capita output from Rennert et al.

TABLE 3.—PERCENTILES OF PREDICTIVE DISTRIBUTIONS FOR AVERAGE GROWTH OVER NEXT 50 AND 100 YEARS: POPULATION WEIGHTED AVERAGE OF COUNTRY GROWTH RATES, 2017

	Percentiles: 50-year horizon			Percentiles: 100-year horizon		
	0.17	0.50	0.84	0.17	0.50	0.84
Global factor (f_t)	0.92	1.86	2.70	0.92	1.87	2.72
	Global aggregates					
All countries	1.03	2.05	3.00	1.06	2.04	2.96
OECD	0.74	1.69	2.62	0.79	1.73	2.62
Non-OECD	1.05	2.13	3.11	1.11	2.10	3.04

Table F-4. Estimate of the distribution of trend growth (σ_m) from MSW.

Note that the estimates of the uncertainty of the growth rate are reasonably consistent across the different approaches and studies.

Additionally, we look at a simple econometric forecast of future growth rates using the combined IMF and Maddison estimates for 1950 – 2022. We use four different specifications for projecting the global growth rate, g_t. For each, we fit over the 1950 – 2022 period and then forecast using dynamic forecasts through 2200. For example, in equation (*Spec* 1), the estimate of the coefficient is α = 2.15 ± 0.179. If we calculate the forecast errors to 2100, they produce an error in the log level of output of 1.62. Converting this to the standard deviation of the growth rate, this yields 0.019% points per year in Table F-5.

$$(Spec\ 1) \quad g_t = \alpha + \varepsilon_t$$

$$(Spec\ 2) \quad g_t - g_{t-1} = \alpha + \varepsilon_t$$

$$(Spec\ 3) \quad g_t = \alpha + \beta g_{t-1} + \varepsilon_t$$

$$(Spec\ 4) \quad TSLS: g_t = \alpha + \beta g_{t-1} + \varepsilon_t$$

Table F-5 shows the forecast standard errors of the growth rates from the estimates. They are substantially lower than the techniques shown in Table F-2, but these are overly simple specifications compared to the techniques in Muller et al. Also, perhaps the last seven decades were a tranquil period.

From 2020 to	Spec 1	Spec 2	Spec 3	Spec 4
2050	0.051	0.454	0.297	0.297
2100	0.019	0.332	0.216	0.216
2150	0.012	0.299	0.194	0.194
2200	0.008	0.283	0.184	0.184

Table F-5. Standard errors of forecasts using global growth rates, 1950 – 2022, in percentage points per year[vii]

Part G. **Dual Discounting**

The macroeconomic structure of the DICE model poses difficulties because it has two alternative discount rates, the first on standard capital and the second on climate investments. Because the discount rate on climate investments is the same as that on standard investments in current DICE model (which we call a one-stage approach), we describe in this section a two-stage investment strategy to determine the difference from the one-stage investment strategy. The concern is that the approach used in the model implicitly adopts the same beta for general and climate investments, despite their empirically different risk properties.

In order to gauge the quantitative importance of this simplification, we run a "dual discounting" version of the model which first optimizes only savings rates with the β parameter in equation (A-6) in Part A set to 1 as is most appropriate for general capital investments. In this first stage, emissions control rates are set at their baseline values. In a second stage run, we then fix savings rates at the optimized level from the first stage and optimize over mitigation rates with $\beta^{clim} = 0.5$ as is appropriate for climate investments. This can be done either with a base or an optimal scenario for calculating the optimal savings rate with β = 1, but the resulting optimal savings rates ratios differ only by a miniscule amount.

Figures G-1 through G-3 show the key results obtained from dual discounting. The optimized control rate, temperature trajectory, and social cost of carbon are slightly different between the one-stage ("benchmark") and the two-stage ("dual discounting") estimates. With dual discounting, the investment rates, emissions-control rates, and output levels are all lower than with the one-stage approach. Because of lower output and emissions, the year 2100 atmospheric temperature is lower with dual discounting: 2.58 °C in the one-stage discounting compared to 2.55 °C in the dual discounting. While the differences between the two approaches are small, the sign of the impact on warming may be surprising.

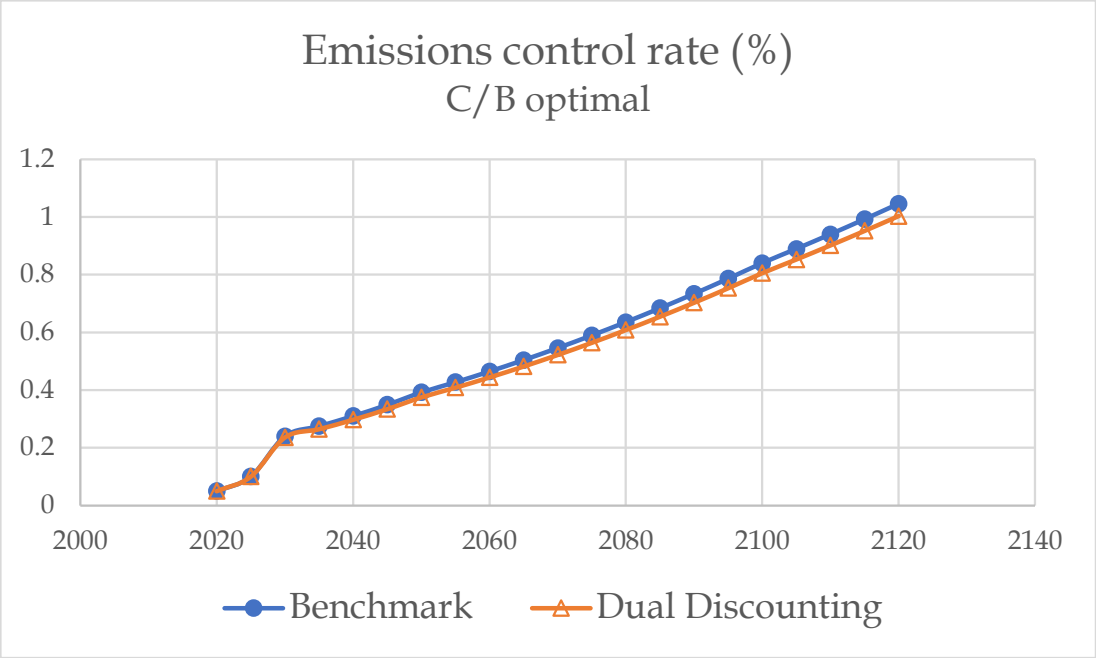

Figure G-1: Emissions control rates in the C/B optimal scenario with the benchmark and dual discounting approaches

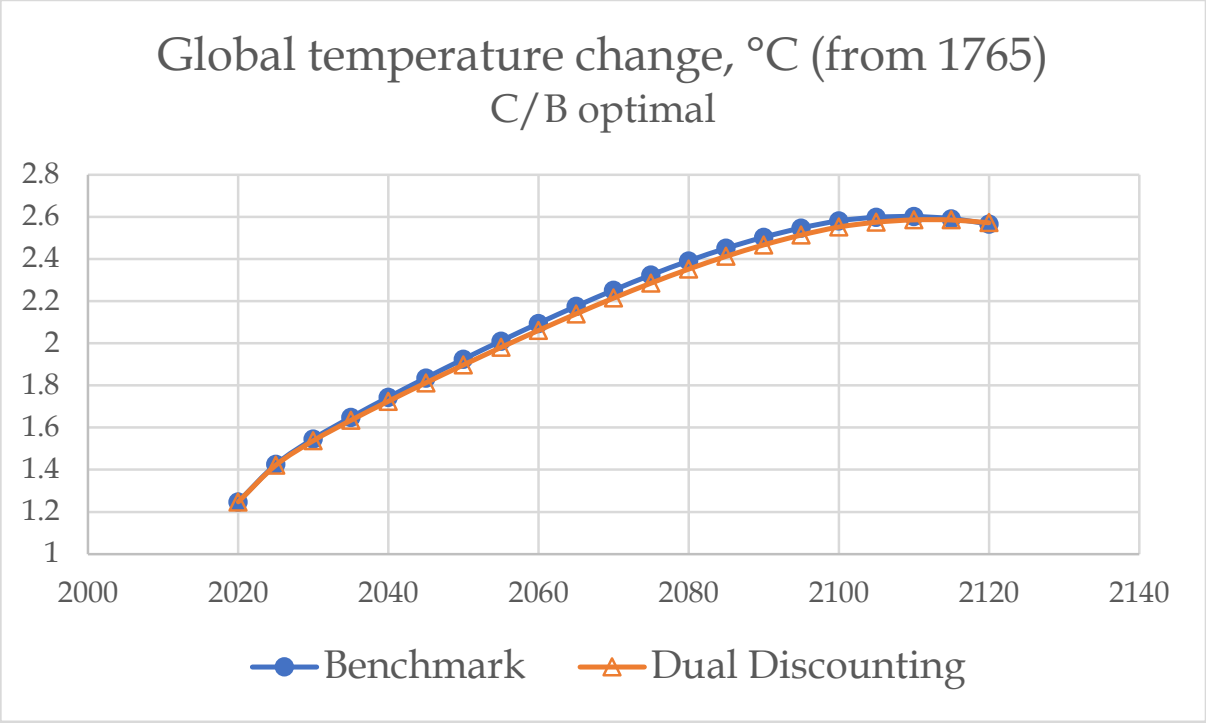

Figure G-2: Global temperature change in the C/B optimal scenario with the benchmark and dual discounting approaches

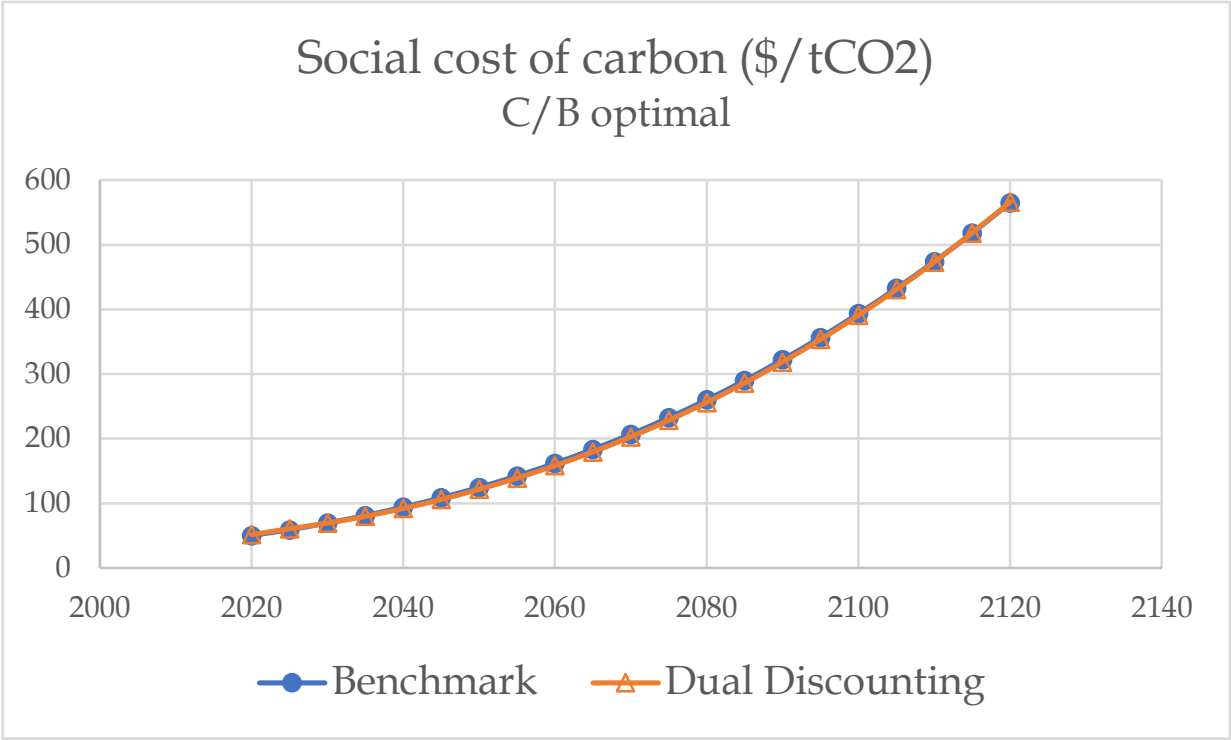

Figure G-3: Social cost of carbon in the C/B optimal scenario with the benchmark and dual discounting approaches

Part H. References

Christensen, Peter, Kenneth Gillingham, and William Nordhaus. 2018. "Uncertainty in forecasts of long-run economic growth." *Proceedings of the National Academy of Sciences* 115: 5409-5414.

Dietz, Simon, Christian Gollier, and Louise Kessler. 2018. "The climate beta." *Journal of Environmental Economics and Management* 87: 258-274.

Gollier, Christian. 2014. "Discounting and growth." American Economic Review 104: 534-537.

Gollier, Christian. 2016. "Evaluation of long-dated assets: The role of parameter uncertainty." *Journal of Monetary Economics*, 84: 66-83.

Mehra, Rajnish 2008. *Handbook of the equity risk premium*. Elsevier.

Mehra, Rajnish, and Edward C. Prescott.1985. "The equity premium: A puzzle," *Journal of monetary Economics* 15: 145-161.

NAS. 2017. National Academies of Sciences, Engineering, and Medicine. *Valuing Climate Damages: Updating Estimation of the Social Cost of Carbon Dioxide*. Washington, DC: The National Academies Press.

NPP. Newell, Richard G., William A. Pizer, and Brian C. Prest. 2022. "A discounting rule for the social cost of carbon." *Journal of the Association of Environmental and Resource Economists* 9: 1017-1046.

Prest, Brian. "Disentangling the Roles of Growth Uncertainty, Discounting, and the Climate Beta on the Social Cost of Carbon" *RFF Working Paper 23-41.*

Rennert, Kevin, Brian C. Prest, William A. Pizer, et al. 2022. "The social cost of carbon: advances in long-term probabilistic projections of population, GDP, emissions, and discount rates." *Brookings Papers on Economic Activity*, : 223-305.

Ulrich K. Müller, James H. Stock, Mark W. Watson. 2022. "An Econometric Model of International Growth Dynamics for Long-Horizon Forecasting," *The Review of Economics and Statistics,* 104: 857–876.

Weitzman, Martin L. 1998. “Why the Far-Distant Future Should Be Discounted at Its Lowest Possible Rate.” J*ournal of Environmental Economics and Management*, 36 (3): 201–8.

Background Note on Damages
March 12, 2023

Advice on Background Notes for DICE-2023: These background notes are for informational purposes for modelers. They are not intended for publication and are not publication quality. Some of the details are sketched and not derived in detail in this document. They may be cited with the warning, "Background notes are for informational purposes and are not published."

SUMMARY

This note describes the calibration of the damage function for DICE-2023. The DICE-2023 damage function is constructed from three elements:
An updated literature-synthesis estimate of global aggregate warming impacts, suggesting a loss of 1.62% GDP-equivalent impact at 3°C warming over pre-industrial temperatures. An adjustment for tipping points based on estimates from Dietz et al. (2021), adding +1% output loss due to 3°C warming.
A judgmental adjustment for further omitted impacts and uncertainty of +0.5% loss at 3°C warming. Item #1 updates the synthesis of literature damage estimates from Nordhaus and Moffat (2017). The remainder of this note describes this update.

Adjustments to Nordhaus and Moffat (2017) Data

We use the review of global aggregate climate change impact estimates from Nordhaus and Moffatt (2017, "NM") as a starting point. They estimate a base damage function utilizing 38 impact estimates from 25 studies (see Table 1). NM's preferred specification is a weighted quantile regression with weights based on considerations such as study recency and quality. We first make three adjustments to NM's original data:

We reduce the weight given to Cline's (1992) damage estimate for 10°C warming from 0.1 in NM to 0.0. This change is motivated by the speculative nature of the 10°C estimate especially relative to growing literature and understanding of impacts for lower levels of warming.

We reduce the weight given to Dellink (2012) from 1.0 to 0.25 to reflect the fact that our updated review includes a newer version of the ENV-Linkages model in Dellink et al. (2019).

We correct the temperature level corresponding to the Bosello et al. (2012) estimate from a pre-industrial to a 1920-40 temperature baseline to align with the other estimates (from 1.92°C to 1.52°C).

New Estimates added to Nordhaus and Moffat (2017) Data

We next update the NM data by adding estimates of global aggregate climate change impacts that have been published since the NM review. Piontek et al. (2021) presents a review of competing methodologies and recent studies quantifying aggregate impacts of climate change. We utilize their review as a basis for this update. This approach was chosen because Piontek et al. (2021) exhibits good coverage and alignment with a similar recent review by the IPCC.[4] We note that the inclusion criteria for new estimates in our analysis are thus not formally the same as for the original NM review.

We specifically consider the studies listed in Piontek et al.'s (2021) Supplementary Materials Table (Section 3). Among these, we focus our attention on new bottom-up and top-down aggregate damage assessments. That is, we exclude studies which use prior impact estimates to propose new damage functions but do not themselves produce new climate change impact estimates. We further restrict our attention to studies that are published and provide estimates of aggregate climate change impacts at the global level. We also exclude one study for which we were unable to replicate temperature projections and received no reply to an inquiry with the corresponding author. These restrictions leave us with 11 new studies from which we extract 18 new estimates as shown in Table 1 below.

We note as well that these estimates differ from those in Howard and Sterner (2017, 2022) used as our alternative damage estimates. Our reservations on the estimates in the 2017 study are that it did not weight studies and additionally it included studies that, in our view, were not empirically based. The new study has not published when the current estimates were prepared, and we will review those when completed.

A. Temperature Baseline Harmonization Notes

The following are general procedures for our estimates:

We harmonize all impact estimates' corresponding temperatures to a 1920-40 baseline so as to align with the original NM data.

[4] The IPCC's 6th Assessment Report presents a synthesis of "Global aggregate economic impact estimates by global warming level" in Figure Cross-Working Group Box ECONOMIC.1 (O'Neill et al., 2022). Our updated damage function includes all studies listed in this Figure except for two review-based estimates (Tol 2018 and Howard and Sterner 2017, where the latter is still considered in our analysis in the "alt. damages" scenario) and two studies that are arguably not independent from other prior literature that is included in the damage function (specifically Burke et al. (2018) which builds on Burke et al. (2015) and Rose et al. (2017) which builds on DICE, PAGE, and FUND).

We generally use warming estimates from within papers when available, including for adjustments to alternate baselines. Otherwise, we assume 0.4 °C warming between 1920-40 and pre-industrial, and use an average of GISS, Hadley, and NCDC temperature anomaly series to infer warming between additional periods as needed (0.5 °C warming between 1980-2004 and 1920-40, 0.55 °C warming between 1985-2005 and 1920-40, 0.56 °C warming between 1980-2010 and 1920-40, and 1.05 °C warming from 1920-40 and 2015-19).

We note that the data sources used for temperature adjustments matter: RCP 8.5 warming in 2100 may be considered as 3.91 °C or 4.25 °Cover 1920-40 levels depending on whether one uses IPCC or the three-averaged data series, for example. These differences will affect the estimated damage function as well.

B. Weights

In line with the NM approach, we also consider weights for each of the new estimates based on our evaluation of each estimate's quality, novelty, and independence (see study notes below). We note that there is not one unique way to construct such weights and that one could create reasonable alternative weighting schemes (including more formal adjustments for considerations such as sectoral coverage of each underlying study). While we prefer the weighted regressions, we also show results for unweighted regressions (Table 2). Both weighted and unweighted regressions yield results of the same order of magnitude but estimates for weighted impacts are generally larger.

C. Updated Data

Study	Year	Temp (°C)	Impact (%)	New	Weight
Cline	1992	2.5	-1.1	0	0.9
Cline	1992	10	-6	0	0
Nordhaus a	1994	3	-1.33	0	0
Nordhaus b	1994	3	-3.6	0	0.5

Nordhaus b	1994	6	-10.4	0	0.5
Frankhauser	1995	2.5	-1.4	0	1
Tol	1994	2.5	-1.9	0	0.1
Nordhaus and Yang	1996	2.5	-1.7	0	0.1
Mendelsohn et al.	2000	2.2	0.03	0	0.1
Mendelsohn et al.	2000	2.2	0.07	0	0.1
Mendelsohn et al.	2000	2	0.08	0	0.1
Mendelsohn et al.	2000	3.5	0.01	0	0.1
Nordhaus and Boyer	2000	2.5	-1.5	0	1
Tol	2002	1	2.3	0	0.1
Maddison	2003	3.1	-2.2	0	0.1
Rehdanz and Maddison	2005	1.24	-0.32	0	0.1
Rehdanz and Maddison	2005	0.84	-0.32	0	0.1
Hope	2006	4.085	-3.04	0	0.25
Nordhaus	2006	3	-1.05	0	1
Nordhaus	2008	3	-2.49	0	0.25
Nordhaus	2010	3.4	-2.8	0	0.25
Maddison and Rehdanz	2011	4	-17.8	0	0.1
Bosello et al.	2012	1.52	0.5	0	1
Ronson and Mensbrugghe	2012	3.1	-2.14	0	0.1
Ronson and Mensbrugghe	2012	5.5	-6.05	0	0.1
Dellink	2012	2.5	-1.1	0	0.25
Kemfert	2012	0.25	-0.17	0	0.1
Hambel	2012	1	-0.3	0	0.1
Nordhaus	2013	3	-2.25	0	0
FUND	2015	2	0.2	0	0.3
FUND	2015	3	-0.17	0	0.4
FUND	2015	4	-0.85	0	0.3
WITCH	2015	2	-1.84	0	0.3
WITCH	2015	3	-3.72	0	0.4
WITCH	2015	4	-6.25	0	0.3
PAGE09	2017	2	-0.72	0	0.3
PAGE09	2017	4	-2.9	0	0.4
PAGE09	2017	6	-6.51	0	0.3
Dellink et al.	2019	2.1	-2	1	0.75
Dellink et al.	2019	3.6	-6	1	0.25
Roson and Sartori	2016	3.55	-1.72	1	0.1
Takakura et al.	2019	2.6	-2.24	1	0.33
Takakura et al.	2019	3.6	-4.69	1	0.33
Takakura et al.	2019	1.6	-1.02	1	0.33
Kompas et al.	2018	3.55	-3	1	0.2
Kompas et al.	2018	4.55	-7.24	1	0.2
Kompas et al.	2018	2.55	-1.77	1	0.2
Zhao et al.	2019	3.1	-2.42	1	0
Letta and Tol	2018	4.412	-1.88	1	0.5

Burke et al.	2015	4.86	-23	1	0.5
Newell et al.	2021	3.91	-2.53	1	1
Pretis et al.	2018	1.6	-13	1	0.35
Pretis et al.	2018	1.1	-8	1	0.15
Kahn et al.	2021	3.91	-7.64	1	1
Kalkuhl and Wenz	2020	4.25	-7.4	1	0.05
Kalkuhl and Wenz	2020	4.25	-13.4	1	0.05

Color Key:	
	Adjusted NM data point
	New bottom-up studies
	New top-down studies

Table 1: Updated data of global climate change impact estimates. “Temp” refers to °C warming over 1920-40 levels. “Impact” refers to estimated global GDP impact in percent. “New” is an indicator equal to 0 for studies already featured in NM and equal to 1 for new studies.

D. Estimation Results

Table 1 summarizes predicted impacts at 3°C and 6°C warming over 1920-40 levels for different data samples and regression specifications (OLS or median, denoted "Qtile"). All estimates are based on a simple quadratic function in temperature (without a constant). We present results for different data samples that exclude damage estimates above certain temperature levels (e.g., “T limit T<10°C” implies that only estimates for less than 10 °C warming are included). The updated preferred estimate – using weighted quantile regression - is highlighted in bold. It suggests around 30% larger impacts (-2.16%) than the corresponding estimate in NM (-1.63%).

			Predicted Impacts at:	
Method	Weights?	T limit	3°C over 1920-40	6°C over 1920-40
OLS	-	-	-1.71%	-6.84%
OLS	-	T<10°C	-2.94%	-11.74%
OLS	-	T<5°C	-3.46%	-13.84%

OLS	Yes	-	-2.94%	-11.74%
OLS	Yes	T<5°C	-3.35%	-13.38%
Qtile	-	-	-1.80%	-7.20%
Qtile	Yes	-	-2.16%	-8.63%

Table 2: Predicted impacts based on updated regression results.

E. Detailed Study Notes

This section describes how impact estimates were extracted from each of the studies added to the NM data, as well as brief notes on weights.

Dellink et al. (2019)

Climate impact projections:

Headline: 2.5 °C warming by 2060 induces average global GDP loss of 2% (by 2060). We infer that the temperature baseline must be preindustrial based on the paper's use of the MAGICC Model and the fact that, in Figure 3, warming levels appear to be 1 °C at 2015.

The paper also makes a damage prediction post 2060. We infer a 6% loss at 4 °C based on the "central projection - full damages" line in Figure 12. Global GDP losses of 2% for 2.1 °C and 6% for 3.6 °C increases over 1920-40 temperature levels.

Weights: 1 total (0.75 on 2.1 °C estimate and 0.25 on 3.6 °C estimate)

Notes: Solid methodology. Put higher weight on the 2.1 °C estimate since the ENV-Linkages model is more detailed and there is more uncertainty about the extrapolation to the AD-DICE model used for the 3.6 °C projection.

Takakura et al. (2019)

Climate impact projections:

Study considers impacts across 4 RCP scenarios x 5 climate models x 5 SSP scenarios.

Temperature baseline is pre-industrial as per SI Figure 2.

We use the paper's Supplementary Information to calculate averages of global impact estimates across years and scenarios for three temperatures of interest: 2 °C warming over preindustrial (by averaging across years and scenarios with warming between 1.98 °C <T<2.02 °C), 3 °C warming over preindustrial (averaging across observations with 2.98 °C <T<3.02 °C), and 4 °C warming over preindustrial (averaging across observations 3.98 °C <T<4.02 °C). We note that we compute aggregate impacts by aggregating the sectoral impacts at the "World" level.

Global GDP losses of 1.02% for 1.6 °C , 2.24% for 2.6 °C , and 4.69% for 3.6 °C over 1920-40 levels.

Weights: 1 total (0.33 on each temperature estimate)

Notes: Independent estimate.

Roson and Sartori (2016)

Climate impact projections:

Paper presents country-level GDP impact estimates for a +3.0 °C increase in average temperature.

The temperature baseline is 1985-2005 for sea level rise, 1980-2004 for agriculture method 2, and not explicitly stated for some of the other impacts, although several infer warming damages relative to current average temperatures. We thus assume a 1985-2005 baseline overall.

No global impact estimate is provided. We constructed one using the country level GDP impact estimates for 3 °C warming presented in Appendix Table A1.1 using 2019 GDP weights (World Bank, PPP, constant 2017 dollars). Note: For countries with missing estimates, we adopt the relevant regional "Rest of Region" estimate (e.g., "Rest of Oceania" for Vanuatu, etc.)

Global GDP loss of 1.72% for 3.55 °C over 1920-40.

Weight: 0.1

Notes: Questions over methodology especially in going from damage functions to GDP impacts.

Zhao et al. (2020)

Climate impact projections:

Damages are reported as the percentage of cumulative discounted climate damages relative to cumulative discounted Gross World Product from 2011-2100. For their "Business as usual" scenario, this percentage is 2.42%. We are inferring associated temperature increase based on Figure 5 as 3.5 °C .

The temperature baseline seems to be preindustrial based on the definition of T variable in equation (3).

Global GDP loss of 2.42% for 3.1 °C warming over 1920-40.

Weight: 0

Notes: Very close to FUND & methodological concerns such as over addition of earthquake and volcano damages in climate impacts.

Kompas et al. (2018)

Climate impact projections:

Project global GDP losses of 3% for 3 °C warming (stated in text).

Temperature baseline is 1985-2005 (confirmed by author in correspondence).

Table A1 gives projected losses in dollars for 4 °C and 2 °C . We calculate the corresponding GDP percentages by backing out the assumed global GDP in 2100 (319.79 trillion). This yields predicted losses of 1.77% for 2 °C and 7.24% for 4 °C over the presumed 1985-2005 baseline.

Global GDP loss of 1.77% for 2.55 °C , 3% for 3.55 °C , and 7.24% for 4.55 °C over 1920-40.

Weight: 0.6 (divided evenly over each estimate)

Notes: Improved methods over but lack of independence from Roson and Sartori (2016).

Kalkuhl and Wenz (2018)

Climate impact projections:

Focus on GRP-weighted aggregate results (Table 7).

Climate impacts are calculated relative to no additional warming beyond 2015-19 base period.

Assume RCP 8.5. The implied average temperature increase from 2015-2019 and 2095-99 is 3.2 °C (population-weighted).

- Cross-sectional estimates imply 7.4% global GRP loss in 2099.
- Panel estimates imply 13.4% global GRP loss in 2099.

Global GDP losses of 7.4% or 13.4% from 3.2 °C +1.05 °C = 4.25 °C over 1920-40 levels.

Weight: 0.1 (divided evenly over each estimate)

We were unable to replicate the data on real output using data for several countries. We are concerned about the study because the damage estimates appear to be based on nominal rather than real output. They will include differences in price levels in the estimates, which is non-standard in damage estimates. This approach was confirmed with the authors.

Kahn et al. (2021)

Climate impact projections:

Their benchmark estimates measure damages relative to a baseline scenario under which temperature in each country continues to increase according to its historical trend from 1960-2014. This is not ideal for our purposes.

For one scenario, the authors also estimate damages relative to a "no warming" beyond 2015 baseline. We use this figure as it is closest to what we want to measure.

The results suggest a global GDP-weighted average income loss of 7.64% in RCP 8.5 by 2100.

As a corresponding temperature increase, we utilize the mean global surface temperature change from RCP 8.5 across models as reported in IPCC (2014), which is 3.7 °C +0.61 °C = 4.31 °C over 1850-1900 levels.

Global GDP losses of 7.64% from 4.31 °C -0.4 °C =3.91 °C over 1920-40.

Weight: 1

Notes: This study has high weight because it uses a different methodology from most other top-down estimates.

Burke et al. (2015)

Climate impact projections:

Headline result is 23% global output loss in 2100 in RCP 8.5 scenario resulting in (population-weighted) average global average temperature change in 2100 of 4.3 °C .

Base period is 1980-2010.

Global GDP losses of 23% for 4.3 °C +0.56 °C = 4.86 °C warming over 1920-40 levels.

Weight: 0.5

Notes: Partial superseded by Newell et al. (2021) and methodological similarities with other top-down estimates.

Pretis et al. (2018)

Climate impact projections:

Compare, relative to a baseline of "no additional warming" over 2006-15 levels, 0.6 °C additional warming or 1.5 over preindustrial, and 1.1 °C additional warming or 2 °C over preindustrial.

Headline numbers:

Median projected global GDP per capita is 8% lower in 2100 for 1.5 °C (imprecisely estimated).

Median projected global GDP per capita is 13% lower in 2100 for 2 °C .

Global GDP loss of 8% for 1.5 °C -0.4 °C = 1.1 °C and 13% for 2 °C -0.4C = 1.6 °C over 1920-40 levels.

Weight: 0.5 (0.35 on 1.6 °C estimate and 0.15 on 1.1 °C estimate)

Notes: Methodological similarities to other top-down estimates. Higher weight on 1.6 °C estimate due to higher statistical precision.

Letta and Tol (2019)

Climate impact projections:

Consider impacts for RCP 8.5 resulting in sample average warming of 3.912 °C over reference period of 1980-2004.

We infer aggregate impacts based on the regression results for the full sample (Table 2 Column 1) and calculate average cumulative impacts, which would suggest 1.88% lower TFP levels by 2095.

Global GDP loss of 1.88% for 3.912 °C +0.5 °C = 4.412 °C over 1920-40.

Weight: 0.5

Notes: Methodological similarities to other top-down estimates.

Newell et al. (2021)

Climate impact projections:

We calculate the mean of the distribution of predicted climate impacts across the bootstrapped "levels effects" models in the MCSs (Figure 6 bottom panel). The authors kindly shared their data for us to be able to perform this calculation.

We focus on the "levels effects" since they are precisely estimated.

The results imply a GDP loss of 2.53% in RCP 8.5 year 2100, which they note to have an associated CMIP5 average warming level of 4.31 °C over pre-industrial.

Global GDP loss of 2.53% from 4.31 °C -0.4C = 3.9 °C over 1920-40 levels.

Weight: 1

Notes: Comprehensive analysis nesting hundreds of potential top-down specifications including those of other studies.

Background Note on DFAIR
October 26, 2023

Advice on Background Notes for DICE-2022: These background notes are for informational purposes for modelers. They are not intended for publication and are not publication quality. Some of the details are sketched and not derived in detail in this document. They may be cited with the warning, "Background notes are for informational purposes and are not published."

I. Summary

This note describes the calibration of the Finite Amplitude Impulse-Response (FAIR) model for DICE-2022, labeled "DFAIR." Part I is the calibration to climate-carbon models. Part II is harmonization with historical data. The appendix shows details from the calculations.

The DFAIR carbon-cycle model differs from the earth-science literature in using a five year step. Otherwise, it is essentially equivalent to the Millar et al. (2017) implementation and tracks closely the adaptation of Dietz et al. (2021). For the climate module, it uses the calibration of Millar et al. (2017) with a simple two-box climate model. We have tested alternative parameterizations. They perform differently for different tests, and we have found the Millar et al. (2017) specification sufficiently close to adopt that for the DFAIR model.

The key findings are the following:

First, the Millar et al. (2017) specification of FAIR tracks closely both carbon cycle models and the historical data on emissions and concentrations. The DFAIR model tends to underestimate concentrations relative to the Joos et al. (2013) multi-model simulations. Additionally, it tends to underpredict concentrations slightly in both the carbon cycle models and for the historical data.

Second, for large pulses (the 5000 GtC pulse estimate by Joos), all versions of the FAIR model behave poorly in the short run (up to 100 years), but they are reasonably close for the longer run.

Third, looking at the two major simulations (100GtC and 5000 GtC), the FAIR model is successful in capturing the saturation in carbon absorption that results in higher atmospheric retention in the large compared

to the small pulse. This is a notable advance over the linear carbon models used in earlier vintages of the DICE and most other IAMs.

The calibration of initial conditions for FAIR is difficult because it is path-dependent. We have created a "1765 model" of the DFAIR GAMS version that runs from 1765 to 2020. Using this, we made a successful splice with the 2020 initial conditions based on the 1765 model.

Fourth, the climate model does a reasonable job of capturing the dynamics and does not need structural revisions from earlier versions of DICE. However, the DFAIR model uses the equation structure of the Millar version, which makes interpretation easier.

Finally, it should be emphasized that the carbon cycle models underlying the multi-model calibrations in Joos et al. (2003) are quite divergent. For example, the 5% - 95% confidence interval for the 100-year time integrated impulse response function for concentrations is 30 – 75 years.

The major open issue is whether the FAIR model's parameters should be adjusted to reflect its shortcomings. This is a larger project and awaits further research.

II. Calibration to climate/carbon cycle models.

The DFAIR model uses the structure derived by Millar et al. (2017), with five year steps. It takes all parameters from the original Millar estimates. The only difference is that the DFAIR model has an equilibrium temperature sensitivity (ETS) of 3.0 °C per CO2 doubling.

We then examined three estimates for the carbon cycle and one test for the climate model. Two of the calibrations were to Joos et al. (2013) multimodel study. Note that according to AR6: "Although there has been greater understanding since AR5 of the carbon cycle responses to CO2 emissions 27 (Chapter 5, Sections 5.4 and 5.5), there has been no new quantification of the response of the carbon-cycle to an instantaneous pulse of CO2 emission since Joos et al. (2013)." Note as well that the models underlying Joos appear to have a neutral biosphere, so that feature misses any interaction with increased carbon uptake in that sector. However, Millar appears to capture land uptake, but the impact of this uptake on parameters is unclear.

A. Carbon cycle

The testing of alternative approaches to the carbon cycle used three pulse tests (100 GtC from pre-industrial conditions, 5000 GtC from pre-industrial conditions, and 100 GtC from 2010 levels) and one run that tested the accuracy of matching historical data on CO2 emissions and concentrations.

i. Pulse tests for 100 GtC from pre-industrial conditions

We began with two pulses from pre-industrial concentrations and compared with Joos et al. (2013). We used the Millar specification of the FAIR model, DFAIR, with five year steps for the comparisons. These tests were not precise for Joos because of the divergence among models. One pulse was 100GtC from pre-industrial conditions (PIC) and the second was 5000GtC from PIC. We also tested alternative parameters to see which would be a better fit (labeled "Best").

Figure 1 shows the key results for the atmospheric retention. The Millar et al. (2017) parameters have lower atmospheric retention than Joos et al. (2013) or the other specifications, particularly at short horizons. The "best" parameters match very closely.

Figure 2 shows the temperature response to the same pulse. The temperature results are reversed, with Millar et al. (2017) having lower temperature than Joos et al. (2013) even though the atmospheric concentrations are lower. This result comes from the difference in the climate models in Joos et al. (2013) and the FAIR 2-equation climate model. There are two versions of Millar. One uses an ETS of 3.0 °C, while the other uses a lower value of 2.75 °C. Both are low relative to the Joos models.

While the temperature models relative to Joos are divergent, the DFAIR version of the climate model matches the IPCC AR6 climate estimates exactly, so this suggests that the problem is the Joos climate models rather than the DFAIR climate model.

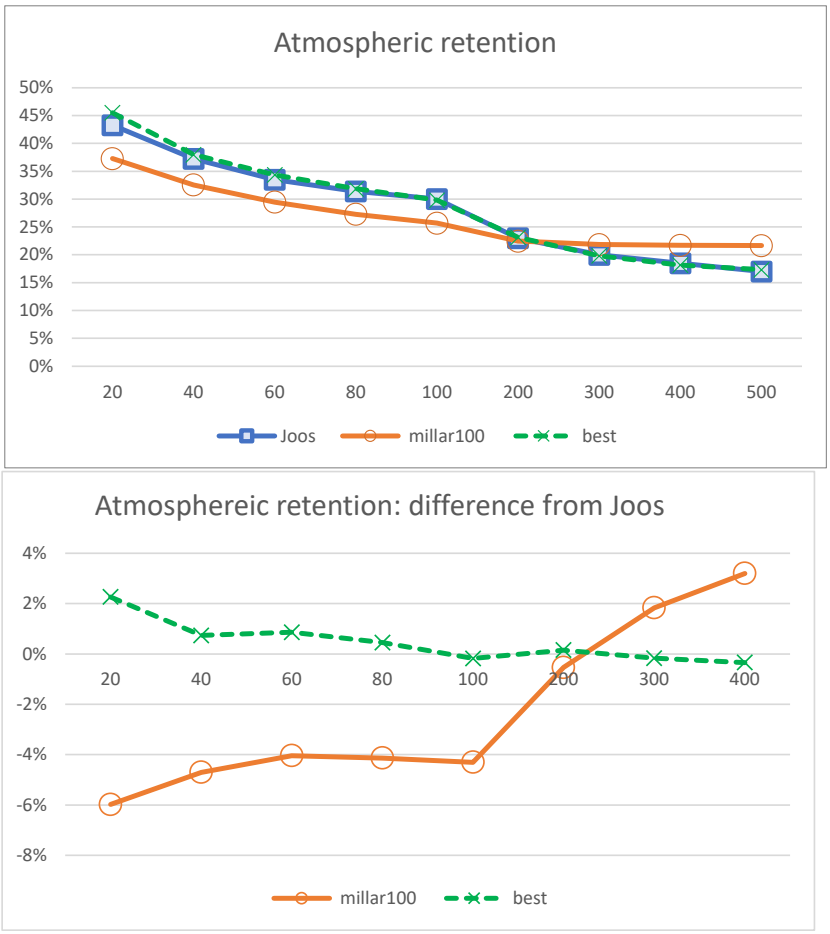

Figure **DFAIR-**1. Atmospheric retention, alternative specifications, pulse of 100 GtC from PIC (years).

(Source: Tests=FAIR-sept0122.xls)

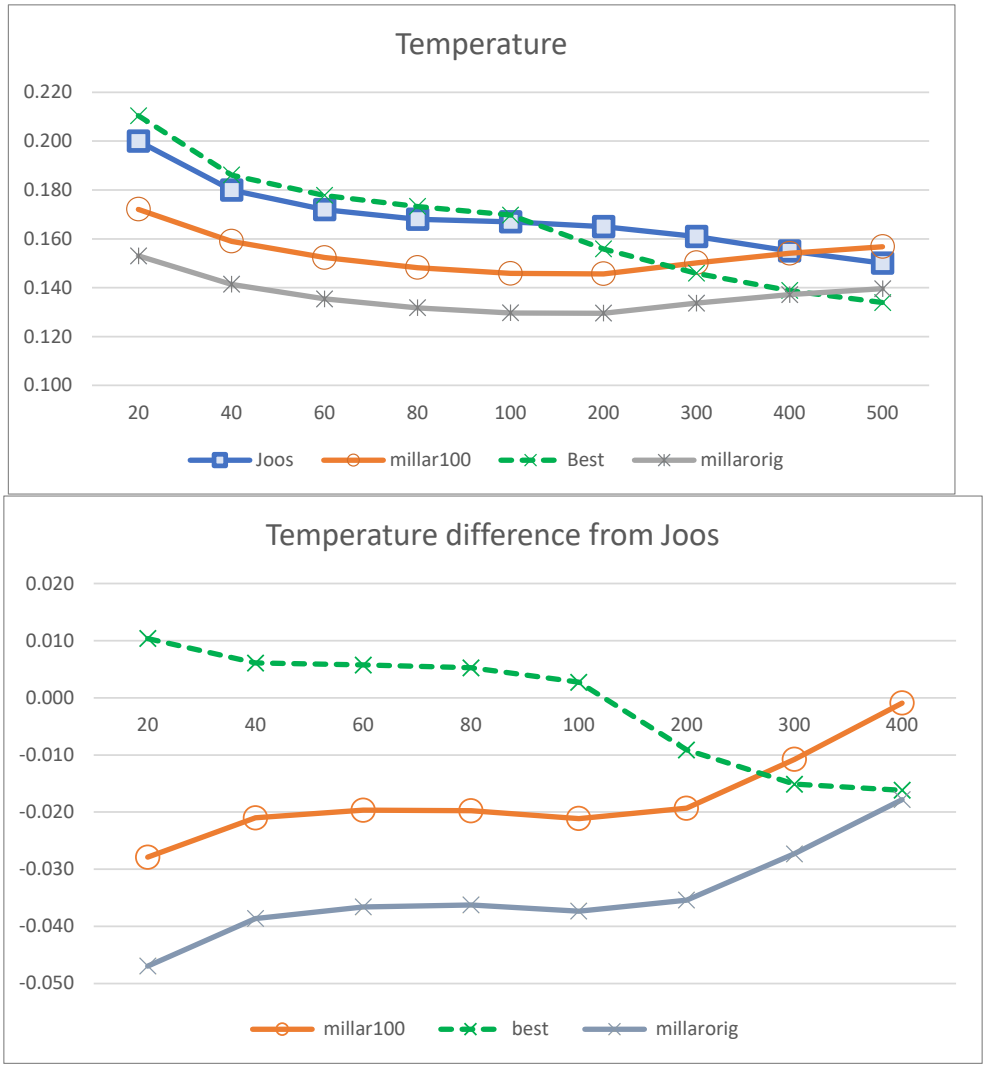

Figure **DFAIR-**2. Results of 100GtC pulse on temperature at different time horizons (years).

(Source: Tests=FAIR-sept0122.xls)

ii. Pulse test for 5000 GtC from pre-industrial conditions

We performed identical runs for a very large pulse, 5000 GtC. For reference, cumulative emissions to date are approximately 2000 GtC by 2100 in the base run and 1400 GtC in the optimal run. The point of this test is to see how well FAIR reproduces the saturation of larger models.

Figure 3 shows the results for the atmospheric retention. FAIR does reasonably well from about 60 years forward, although it tends to have lower convexity than the full earth-system models in Joos et al. (2013). This non-convexity seems to hold for all model parameters, and FAIR therefore tends to understate concentrations for the first half-century (as was the case for the 100 GtC pulse as well). Figure 4 shows the results for temperature (using the higher ETS). The simple climate model fails to capture the shape of the full models after 100 years. The reason for the difference is unclear and is probably not due to the error in the atmospheric retention.

However, the most important result is that the model definitely captures the saturation with high pulses. Note, comparing figures 1 and 3, that the atmospheric retention rises from 30% with the small shock to 70% with the large shock at 100 years. Linear carbon cycle models, such as those used in earlier DICE models and other studies, would have identical percentages.

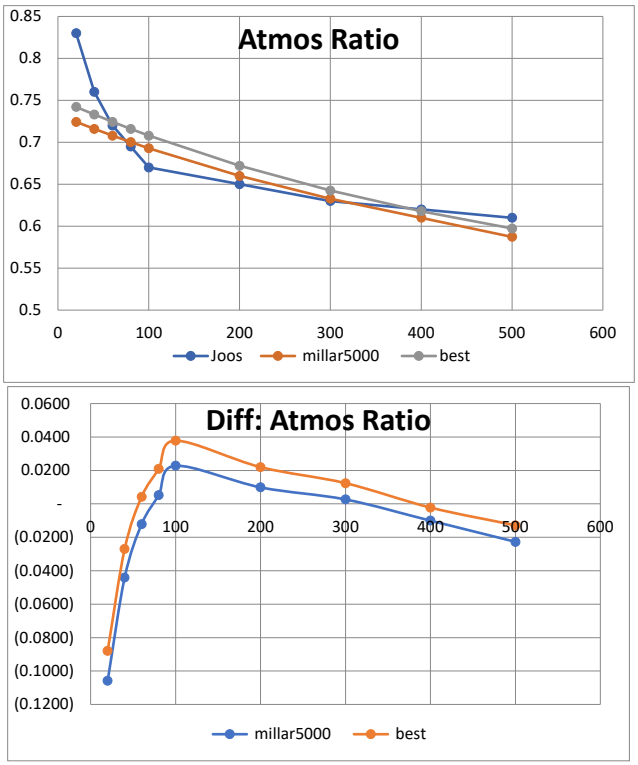

Figure **DFAIR-**3. Atmospheric retention of CO2 for 5000 GtC pulse

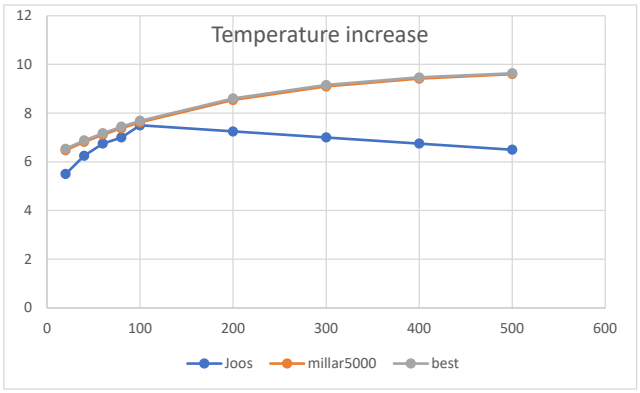

Figure **DFAIR-**4. Temperature increase (°C) for 5000 GtC pulse

iii. <u>100 GtC from 2010 levels (389 ppm)</u>

The third pulse test considered 100 GtC again but against background concentrations which are otherwise held constant at 2010 levels assumed to be 389 ppm (829.42 GtC), in line with both Joos et al. (2013) and the key results reported also in Dietz et al. (2021). For this test, we modify the finel

DFAIR model from DICE-2023 based on the experimental conditions of Joos et al. and Dietz et al. In particular, we (i) follow Dietz et al. in distributing the corresponding initial excess atmospheric CO2 concentrations over pre-industrial levels (829.42 – 588 = 241.4 GtC) into the four carbon reservoirs according to 52.9% in box 1; 34.3% in box 2; 11.1% in box 3; 1.6% in box 4; (ii) assuming 0.85 ◦ C as initial atmospheric warming relative to pre-industrial and lower ocean warming of 0.22°C. (by setting initial temperature in Box 1 to 0.22°C and in Box 2 to 0.63°C so that TATM0 = 0.85°C); (iii) assuming 531 GtC as initial cumulative emissions as in Dietz et al.; (iv) adopting the baseline emissions scenario from Dietz et al. to keep concentrations absent the pulse approximately constant (specifically by adding up annual emissions underlying Dietz et al. into 5-year totals and taking the average per period as value for ECO2); (v) assuming zero non-CO2 forcings as in Dietz et al., noting that experimentation with assuming initial year non-CO2 forcings to be constant at initial year levels had only a minimal impact (+0.001-0.002◦C) on the estimated temperature response. One notable difference from Dietz et al. is that we do not assume an equilibrium climate sensitivity of 3.1°C (which they impose across models) but retain the DFAIR benchmark value of 3.0°C in line with IPCC AR6.

The results of the 100 GtC pulse test in this environment are shown in Appendix Figure D-1. The results indicate that the DFAIR model addresses the critique of Dietz et al. (2021) and others that prior vintages of DICE exhibited excessive warming inertia in response to emissions impulses compared to recent climate model estimates as shown in Joos et al. (2013). It does, however, again also indicate that DFAIR initially underpredicts warming levels slightlyl in the near term, and overpredicts slightly in the longer run.

iv. *Comparison with history*

The final comparison is to use FAIR to project concentrations from 1765 to 2020. For this purpose, we used actual CO2 emissions as best coult be reconstructed from IPCC, CDIAC, and EDGAR. We then constrained both CO2 emissions and non-CO2 forcings using the data from AR6. The emissions were from Table 5.1, while the non-CO2 forcings were from Table AIII.3, and were interpolated. We then ran the model from pre-industrial concentrations starting in 1765.

This specification overpredicted temperature signficantly in 2020 (1.515 °C v. 1.25 °C from IPCC). Additionally, it overpredicted ppm but only slightly (422.5 v 417.1 ppm).

We then created a "1765 run" to match CO2 concentrations. The 1765 run adjusted both emissions and non-CO2 forcings to better track history. This run slightly underpredicted 2020 ppm (414.7 v 417.1 ppm actual) but matched tempeature (1.248). We then used the 2020 values here for calibration of the DICE-2020 model. The following shows the assumptions and results for the different scenarios and history.

		1900	1950	2000	2020
CO2 emissions (GtCO2)					
	Uncalibrated	6.2	11.2	30.0	40.5
	Calibrated	5.4	9.9	30.0	40.5
	IPCC total	3.5	7.6	27.4	36.6
	DICE	2.0	6.2	25.7	37.7
Non-CO2 forcings (W/m2)					
	Uncalibrated	0.00	0.06	0.46	0.68
	Calibrated	-0.10	-0.04	0.06	0.28
	History	-0.01	-0.06	0.46	0.68
Concentrations (ppm)					
	Uncalibrated	291.9	311.6	373.1	422.5
	Calibrated	289.8	306.8	366.7	414.7
	History	295.7	311.3	370.0	414.0
Temperature (from 1765)					
	Uncalibrated	0.19	0.39	1.05	1.52
	Calibrated	0.11	0.29	0.80	1.25
	History	0.13	0.30	0.87	1.25

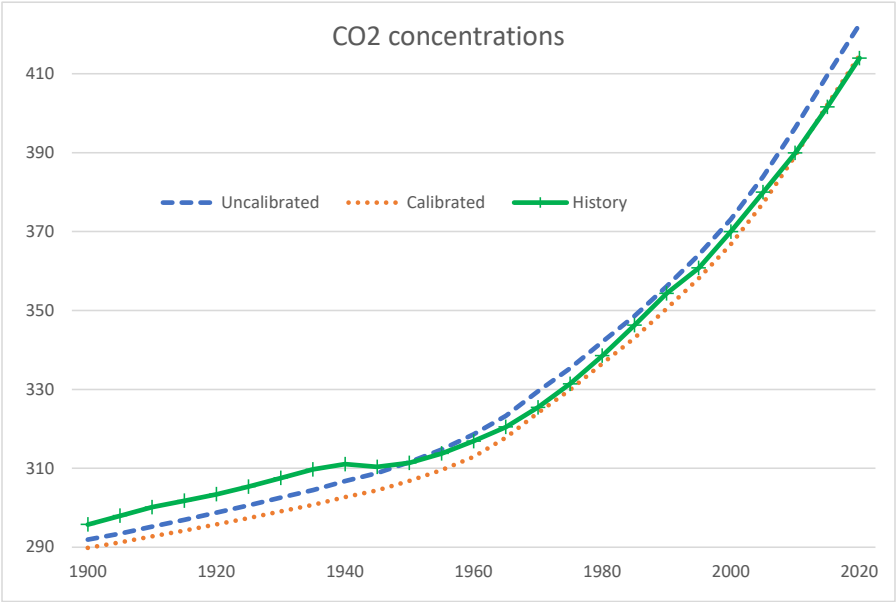

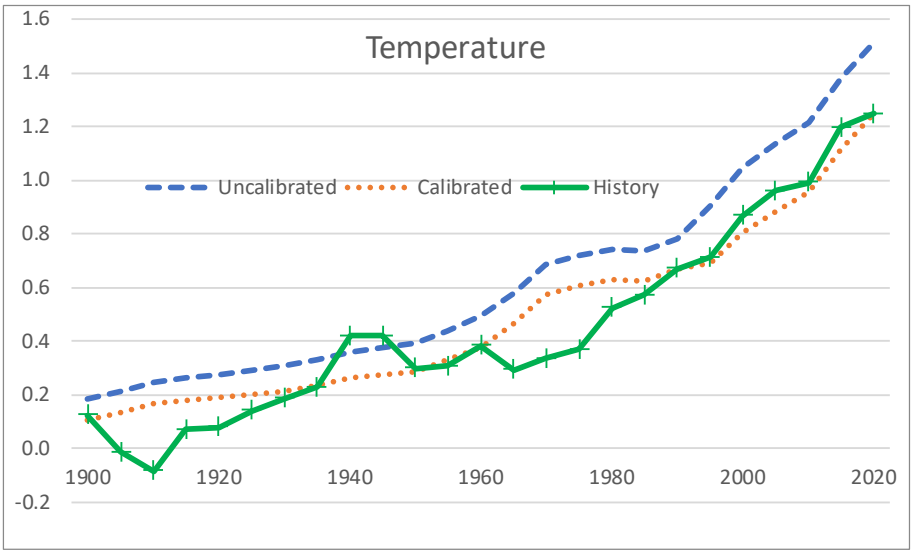

Table DFAIR-1 and Figure DFAIR-5. Comparison of FAIR model variants with history and two scenarios for emissions and forcings

Source: DICE2022A-base-3-11-1765-Runs.xlsx.

B. Climate Module

The FAIR climate module is analytically similar to that in DICE-2016. It is a two-equation model with five parameters (see appendix for the equations). We have adopted four of the five, which represent the dynamics, but have changed the temperature sensitivity from 2.75 °C to 3.0 °C.

We then ran a standard test for the dynamics of the model using stylized CO2 concentrations. This involved 1% concentration growth from pre-industrial concentrations to doubling and then constant concentrations after that. Table 2 shows the transient and equilibrium temperature sensitivity (transient is average around 70 after the start of the growth). The DFAIR does fine here.

	DFAIR	IPCC-AR6
TSC	1.80	1.80
ESC	3.00	3.00

TSC = transitory sensitivity coefficient = temperature increase at 60-80 years
ESC = equilibrium sensitivity coefficient
Units are degrees C from pre-industrial conditions

Table DFAIR-2. Behavior of DFAIR climate module compared to Sixth IPCC Assessment report

[Source: ESC-table-092522u122822.xls]

C. Calibration of history with projections.

The final step is to calculate the initial conditions. (These are listed at the end of this section.) These are the initial stocks in the four carbon reservoirs, cumulative carbon emissions, and the initial temperatures in the two boxes.

To estimate these, we used the "1765 model." This starts in equilibrium in 1765, with all initial stocks in equilibrium. It then puts historical CO2 emissions into the DFAIR model starting in 1765. The simulation uses the calibrated version discussed above.

We then calibrated the DICE model (starting in 2020) with the 1765 model and compared the outputs over the splice period from 2020 to 2035. [update using Millar (adj)]. Table 3 compares the outputs of 1765 model and 2020+ model and shows the splice is essentially perfect.

Period	1	2	3	1
Year	2020	2025	2030	2035
Total CO2 Emissions, GTCO	0.08%	0.48%	1.69%	2.42%
Atmospheric concentration	0.00%	0.02%	0.10%	0.19%
Atmospheric temperaturer	0.00%	0.03%	0.12%	0.26%
Total forcings w/m2	7.72%	0.05%	0.17%	0.34%
Forcings, exogenous w/m2				
CO2 forcings w/m2	0.00%	0.06%	0.20%	0.38%
Total CO2 Emissions, GTCO	0.08%	0.48%	1.69%	2.42%
Permanent C box	0.00%	0.04%	0.15%	0.29%
Slow C box	0.00%	0.06%	0.21%	0.41%
Medium C box	0.00%	0.15%	0.57%	1.06%
Fast C box	0.00%	0.42%	1.49%	2.34%
Temp Box 1	0.00%	0.01%	0.03%	0.06%
Temp Box 2	0.00%	0.03%	0.13%	0.28%
Alpha	0.00%	-0.02%	-0.03%	0.06%
IFR	0.00%	0.00%	-0.01%	0.01%
cacc	0.00%	-0.05%	-0.14%	-0.14%
ccatot	0.00%	0.01%	0.04%	0.15%

Table DFAIR-3. Quality of splice between 1765 model and DICE model.

Percentage difference between the values of 1765 model and DICE-2022 for overlap of splice.

[Source: compare-1765-dice2022-u122822.xls]

The following are the initial conditions for the calibrated version (note that the high resolution figures are from the output of the 1765 model). One important note is that the temperature change is from 1765 and therefore does not always match either the standard calculations from preindustrial or those in damage studies.

```
** INITIAL CONDITIONS TO BE CALIBRATED TO HISTORY
** CALIBRATION
    mat0   Initial concentration in atmosphere in 2020 (GtC)     /886.5128014/

    res00  Initial concentration in Reservoir 0 in 2020 (GtC)      /150.093 /
    res10  Initial concentration in Reservoir 1 in 2020 (GtC)      /102.698 /
    res20  Initial concentration in Reservoir 2 in 2020 (GtC)      /39.534  /
    res30  Initial concentration in Reservoir 3 in 2020 (GtC)      / 6.1865 /

    mateq      Equilibrium concentration atmosphere  (GtC)          /588   /
    tbox10    Initial temperature box 1 change in 2020 (C from 1765)  /0.1477  /
    tbox20    Initial temperature box 2 change in 2020 (C from 1765)  /1.099454/
    tatm0     Initial atmospheric temperature change in 2020         /1.24715 /
```

Appendix DFAIR-1. Parameters of different models.

The basic parameters from Millar et al. (2017) are reproduced in Table A-1.

Table 1. Default parameter values for the simple impulse-response climate–carbon-cycle models used in this paper.

Parameter	Value – AR5-IR	Value – PI-IR	Value – FAIR	Guiding analogues
a_0	0.2173	0.1545	0.2173	Geological re-absorption
a_1	0.2240	0.1924	0.2240	Deep ocean invasion/equilibration
a_2	0.2824	0.2424	0.2824	Biospheric uptake/ocean thermocline invasion
a_3	0.2763	0.4108	0.2763	Rapid biospheric uptake/ocean mixed-layer invasion
τ_0 (year)	1×10^6	1×10^6	1×10^6	Geological re-absorption
τ_1 (year)	394.4	276.7	394.4	Deep ocean invasion/equilibration
τ_2 (year)	36.54	30.75	36.54	Biospheric uptake/ocean thermocline invasion
τ_3 (year)	4.304	4.459	4.304	Rapid biospheric uptake/ocean mixed-layer invasion
q_1 ($KW^{-1}\,m^2$)	0.33	0.33	0.33	Thermal equilibration of deep ocean
q_2 ($KW^{-1}\,m^2$)	0.41	0.41	0.41	Thermal adjustment of upper ocean
d_1 (year)	239.0	239.0	239.0	Thermal equilibration of deep ocean
d_2 (year)	4.1	4.1	4.1	Thermal adjustment of upper ocean
r_0 (year)	–	–	32.40	Preindustrial $iIRF_{100}$
r_C (year GtC^{-1})	–	–	0.019	Increase in $iIRF_{100}$ with cumulative carbon uptake
r_T (year K^{-1})	–	–	4.165	Increase in $iIRF_{100}$ with warming

Table DFAIR-A-1. Parameters in Millar version of FAIR model.

(Source: Millar et al. (2017) , Table 1)

Appendix DFAIR-2. Parameters of Millar Model and Alternatives

Parameters	Millar (orig)	Dietz	DFAIR
emshare0	0.2173	0.2173	0.2173
emshare1	0.2240	0.2240	0.2240
emshare2	0.2824	0.2824	0.2824
emshare3	0.2763	0.2763	0.2763
tau0	1,000,000	1,000,000	1,000,000
tau1	394.4000	394.4000	394.4000
tau2	36.5300	36.5300	36.5300
tau3	4.3040	4.3040	4.3040
teq1	0.3300	0.3300	0.3240
teq2	0.4100	0.4100	0.4400
d1	239.0000	239.0000	236.0000
d2	4.1000	4.1000	4.0700
IRF0	32.4000	34.4000	32.4000
irC	0.0190	0.0190	0.0190
irT	4.1650	4.1650	4.1650
fco22x	3.7400	4.2000	3.9300
mat0	588.0000	588.0000	588.0000

Variable	Units	Definition
emshare0	Fraction	Geological re-absorption
emshare1	Fraction	Deep ocean invasion/equilibration
emshare2	Fraction	Biospheric uptake/ocean thermocline invasion
emshare3	Fraction	Rapid biospheric uptake/ocean mixed-layer invasion
tau0	Year	Geological re-absorption
tau1	Year	Deep ocean invasion/equilibration
tau2	Year	Biospheric uptake/ocean thermocline invasion
tau3	Year	Rapid biospheric uptake/ocean mixed-layer invasion
teq1	$KW^{-1}m2$	Thermal equilibration of deep ocean
teq2	KW-1m2	Thermal adjustment of upper ocean
d1	Year	Thermal equilibration of deep ocean
d2	Year	Thermal adjustment of upper ocean
IRF0	Year	Preindustrial iIRF100
irC	$YearGtC^{-1}$	Increase in iIRF100 with cumulative carbon uptake
irT	$YearK^{-1}$	Increase in iIRF100 with warming
fco22x	$KW^{-1}m2$	Forcings for CO2 doubling
mat0	GtC	Initial carbon stock

Appendix DFAIR-3.. Literature on Carbon Cycle

The following show the results from the Joos et al. (2013) study that are used in the calibrations discussed above.

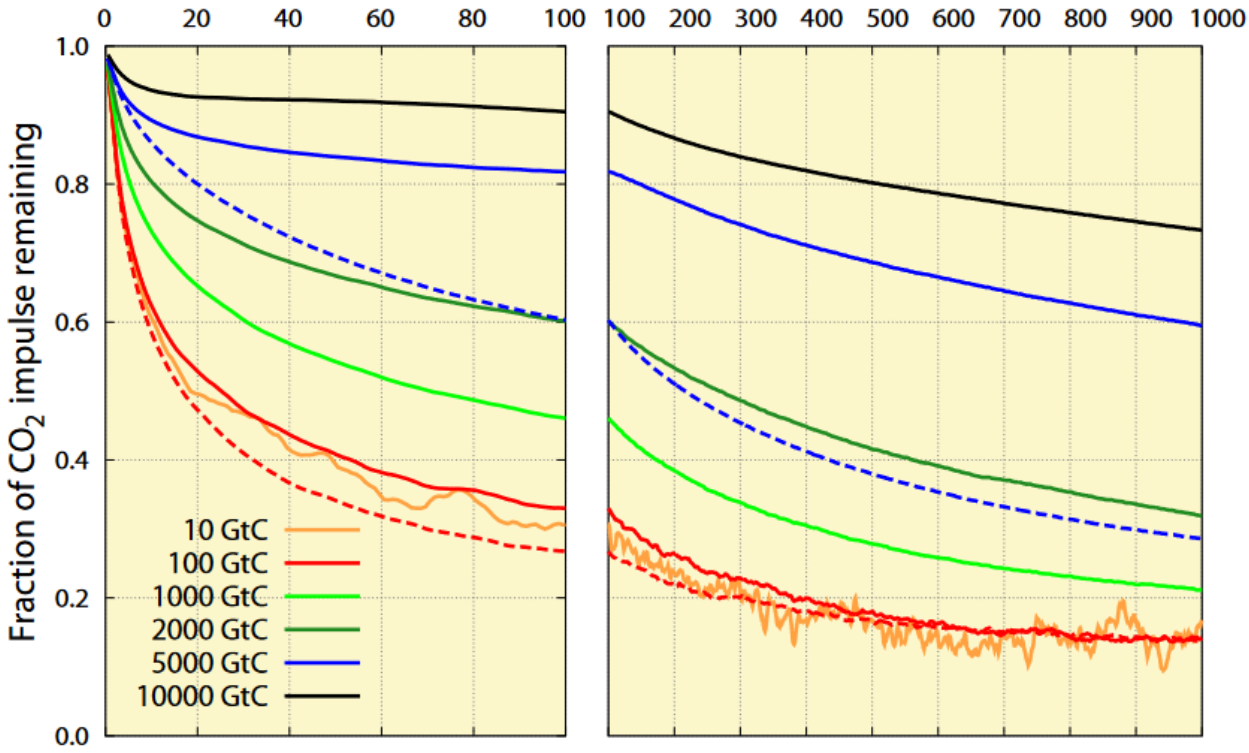

[From Joos et al. (2013): "Fig. 7. Influence of pulse size and climate-carbon cycle feedback on the response in atmospheric CO2 and the time-integrated IRFCO2 as simulated with the Bern3D-LPJ model (standard setup). Pulse emissions, ranging from 10 to 10 000 GtC in the individual simulations, are added to the atmosphere under preindustrial conditions. Dashed lines represent simulations where climate was kept constant in the model."]

A. Results for atmospheric retention of pulses in multimodel:

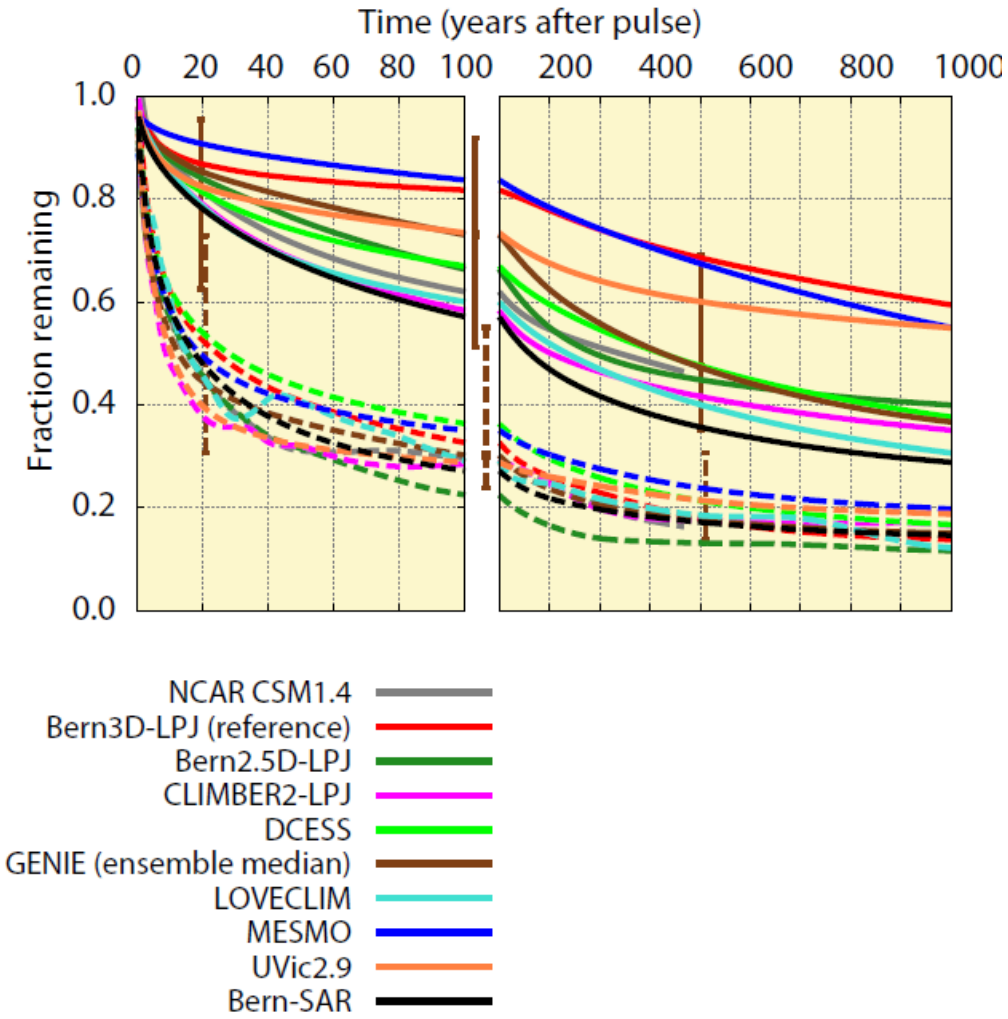

[From Joos et al. (2013): " Fig. 6. Response of the carbon cycle-climate system to a pulse emission of 5000 GtC (solid, PI5000) and 100 GtC (dashed, PI100) added to the atmosphere under preindustrial conditions. The responses in surface air temperature, ocean heat content, steric sea level rise, and in carbon fluxes for PI5000 are scaled by a factor of 50 for a better comparison with the 100 GtC pulse."]

B. Results for temperature to pulses

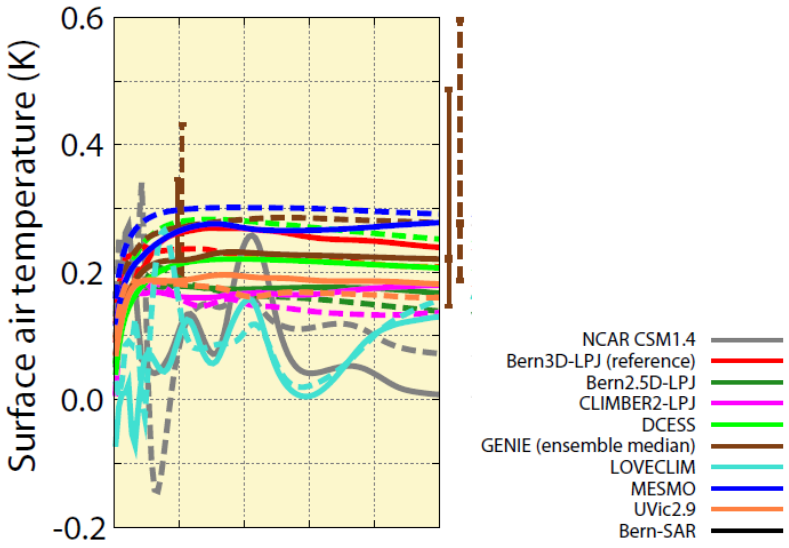

"From Joos et al. (2013): Fig. 4. Influence of the background conditions on the climate-carbon cycle response to a pulse emission of 100 GtC into the atmosphere. Solid lines are for current conditions (CO2, ref = 389 ppm, PD100) and dashed lines for preindustrial conditions (CO2, ref = 280 ppm, PI100)."

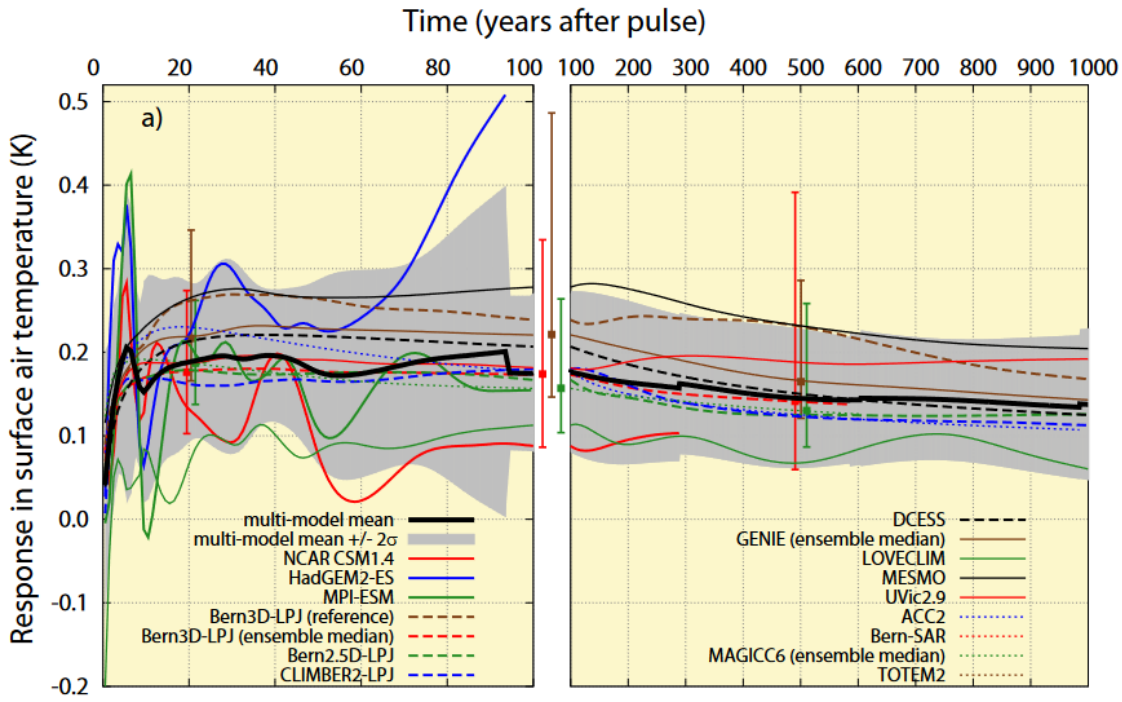

[From Joos et al. (2013): "Fig. 2. As Fig. 1 but for the perturbation in global mean surface air temperature (a), in ocean heat content (b), and in steric sea level rise (c). Results are for a CO2 emission pulse of 100 GtC added to a current CO2 concentration of 389 ppm (PD100).We note that the signal-to-noise ratio is small for the models that feature a dynamic atmosphere (HadGEM2-ES, MPI-ESM, NCAR-CSM1.4, and LOVECLIM) and the plotted evolutions for these models represent both the forced response and a contribution from the models' internal (unforced) climate variability. Small abrupt changes in the multi-model mean and confidence range arise from a change in the number of model simulations; different groups run their model over different periods, pending on CPU availability."]

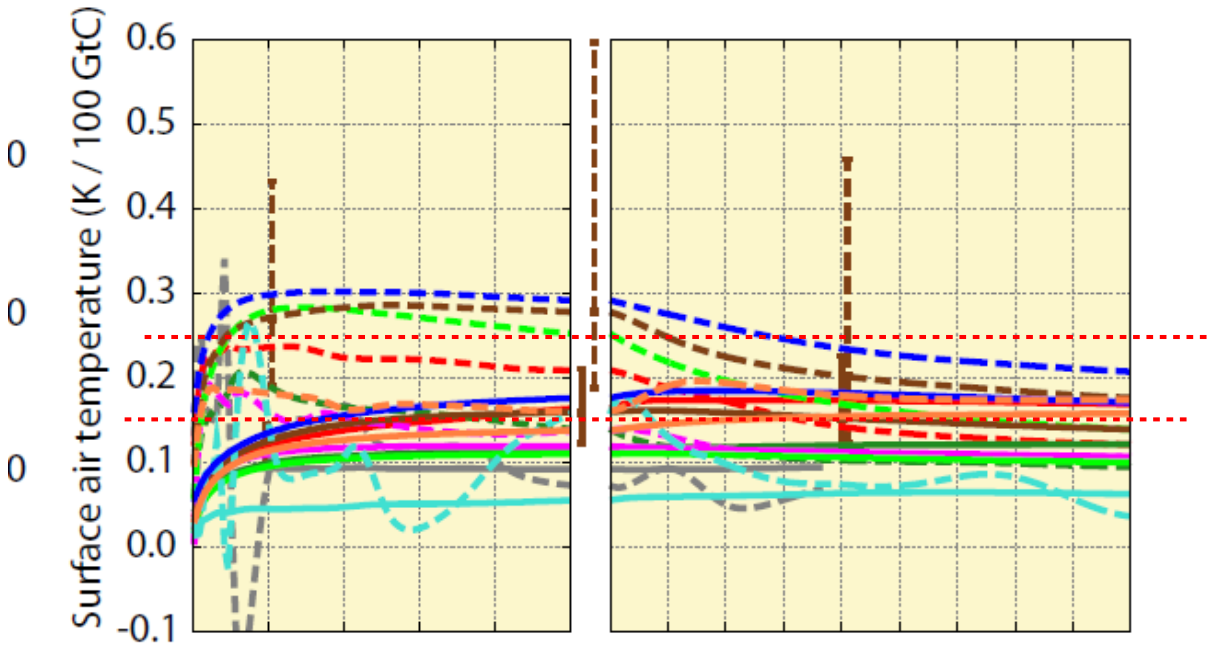

[From Joos et al. (2013): "Fig. 6. Response of the carbon cycle-climate system to a pulse emission of 5000 GtC (solid, PI5000) and 100 GtC (dashed, PI100) added to the atmosphere under preindustrial conditions. The responses in surface air temperature, ocean heat content, steric sea level rise, and in carbon fluxes for PI5000 are scaled by a factor of 50 for a better comparison with the 100 GtC pulse."]

NOTE that Millar et al. (2017) finds roughly the same results in his comparison.

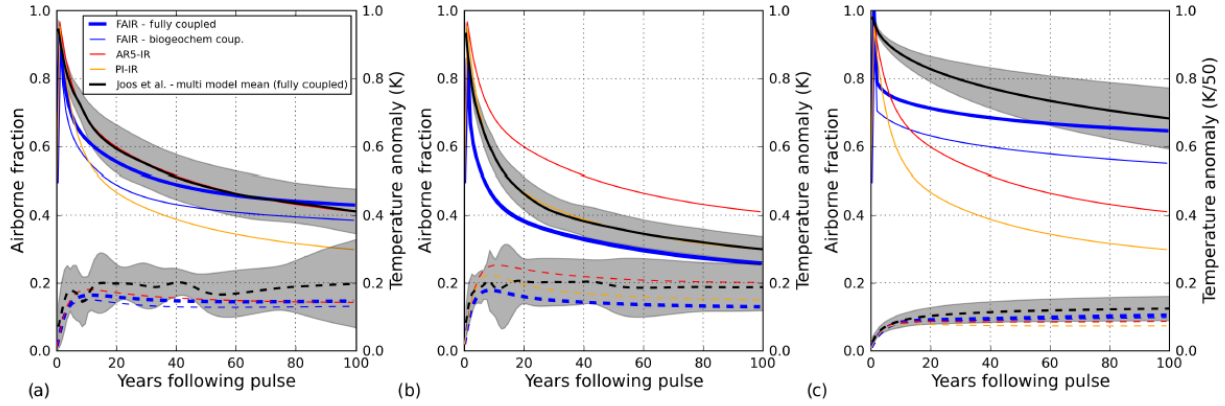

Figure 3. Response to pulse emission experiments of Joos et al. (2013). **(a)** shows the response to a 100 GtC imposed on present-day (389 ppm) background conditions (PD100 experiment), **(b)** the response to a 100 GtC pulse in preindustrial conditions (PI100 experiment) and **(c)** the response to a 5000 GtC pulse in preindustrial conditions (PI5000 experiment) with the warming normalised by the increase in pulse size between **(b)** and **(c)**. Airborne fraction (left-hand axis) is represented by solid lines in all panels and warming (right-hand axis) by dashed lines. FAIR is shown as thick blue lines, AR5-IR as red, and PI-IR as orange. The black lines in all panels shows the Joos et al. (2013) multi-model mean for airborne fraction (solid) and warming (dashed), with the grey shading indicating 1 standard deviation uncertainty across the ensemble. Thin blue lines denote the biogeochemically coupled version of FAIR.

Following is blowup of (b), 100GtC from preindustrial.

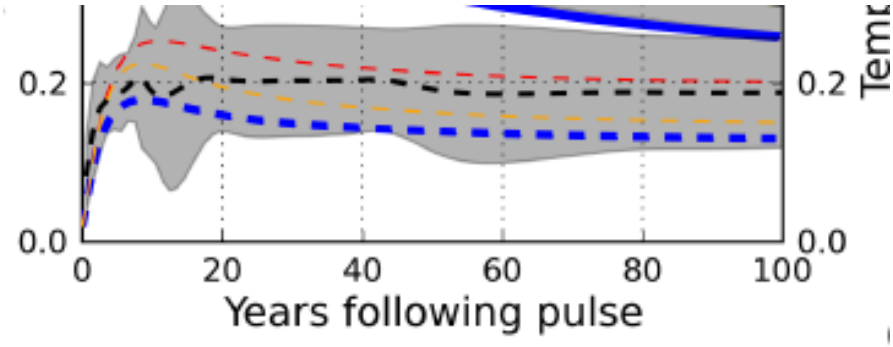

Although there is little discussion of the basic carbon cycle in IPCC AR6, there is discussion of the asymmetry. Figure 5.35 from IPCC AR6 is consistent with the Joos et al. (2013) findings. Median model is 30% retention for a 100GtC pulse from PI conditions.

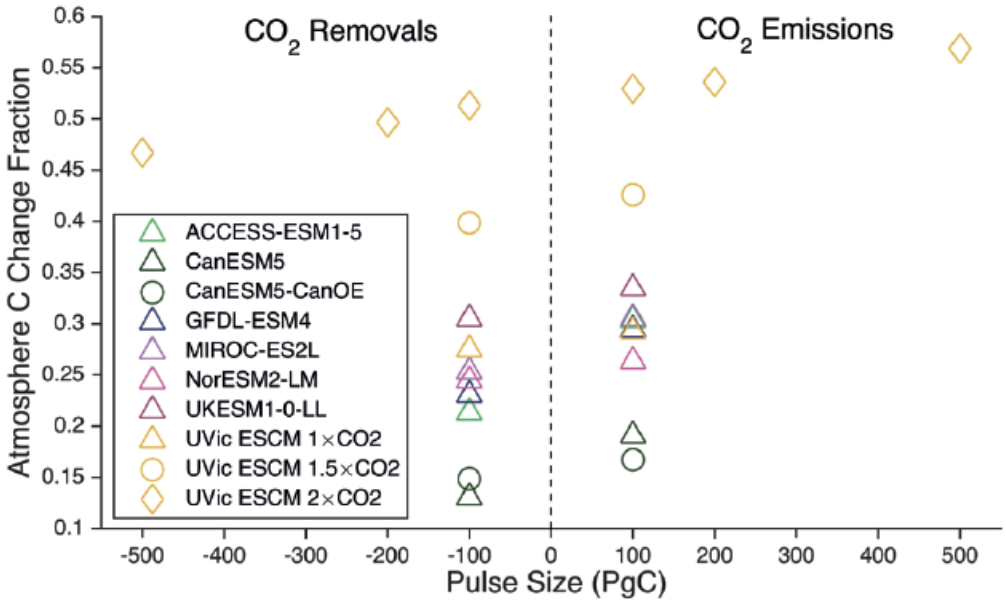

"Figure 5.35 | Asymmetry in the atmospheric carbon dioxide (CO2) response to CO2 emissions and removals. Shown are the fractions of total CO2 emissions remaining in the atmosphere (right-hand side) and CO2 removals remaining out of the atmosphere (left-hand side) 80–100 after a pulse emission/removal. Triangles and green circles denote results for seven Earth system models (ESMs) and the UVic ESCM model of intermediate complexity forced with ±100 PgC pulses applied from a pre-industrial state (1 × CO2) (Carbon Dioxide Removal Model Intercomparison Project (CDRMIP) experiment CDR-pi-pulse; Keller et al., 2018b). Yellow circles and diamonds indicate UVic ESCM results for CO2 emissions/removals applied at 1.5 times (1.5 × CO2) and 2 times (2 × CO2) the pre-industrial CO2 concentration, respectively. Pulses applied from a 2 × CO2 state span the magnitude ±100 PgC to ±500 PgC. UVic ESCM data is from Zickfeld et al. (2021). Further details on data sources and processing are available in the chapter data table (Table 5.SM.6)."

Median model is 30% retention for a 100GtC pulse from PI conditions.

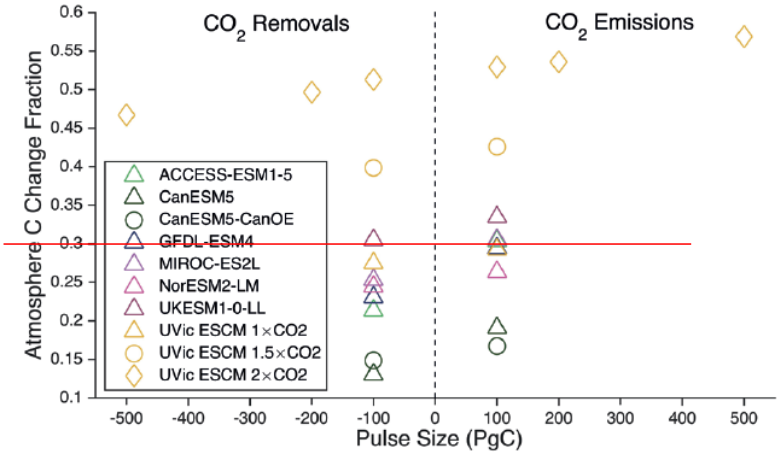

Same as Joos et al. (2013) below:

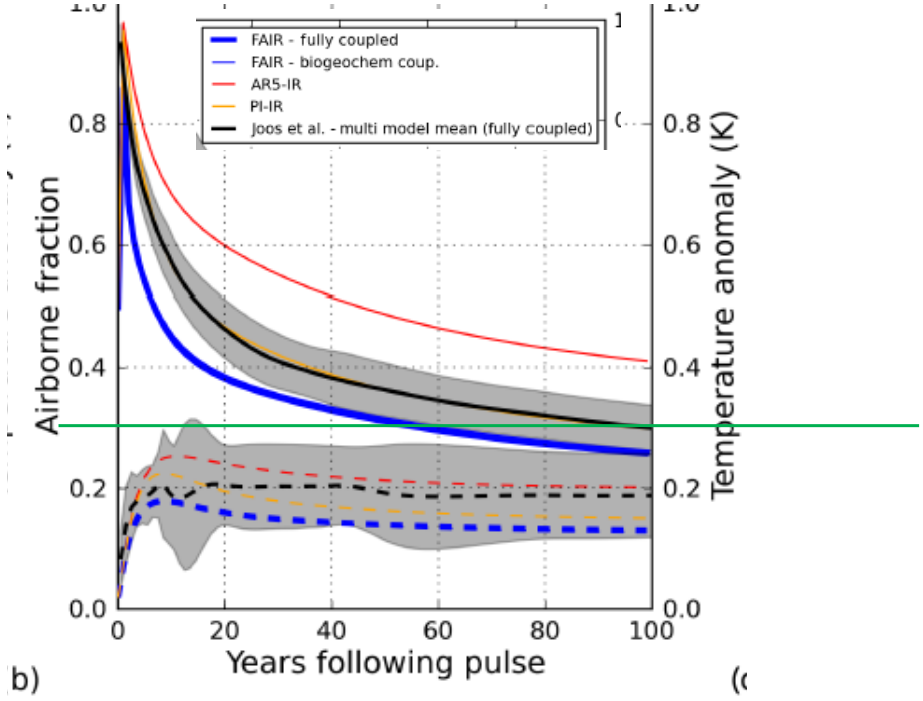

NOTE from AR6: "Although there has been greater understanding since AR5 of the carbon cycle responses to CO2 emissions 27 (Chapter 5, Sections 5.4 and 5.5), there has been no new quantification of the response of the carbon-cycle 28 to an instantaneous pulse of CO2 emission since Joos et al. (2013)."

So, best is to start with calibrating to the 100 year, 100GtC pulse. Here are parameters for best (v1), Millar et al. (2017) , and others. The adjustments necessary are both (1) decrease the permanent share by about .05; and (2) increase the IFR0 by about 7 years. The latter was used by Dietz et al, and the former is necessary to get the asymptote correct.

Parameters		millar100	v1	v2	v3	v4
emshare0 =		0.2173	0.1650	0.1650	0.2173	0.1650
emshare1 =		0.2240	0.2740	0.3040	0.2240	0.2240
emshare2 =		0.2824	0.3324	0.3824	0.2824	0.3824
emshare3 =		0.2763	0.2286	0.1486	0.2763	0.2286
tau0 =		1.00E+06	1.00E+06	1.00E+06	1.00E+06	1.00E+06
tau1 =		394.4000	394.4000	394.4000	394.4000	394.4000
tau2 =		36.5300	36.5300	36.5300	36.5300	36.5300
tau3 =		4.3040	4.3040	4.3040	4.3040	4.3040
teq1 =		0.3300	0.3300	0.3300	0.3300	0.3300
teq2 =		0.4100	0.4100	0.4100	0.4100	0.4100
d1 =		239.0000	239.0000	239.0000	239.0000	239.0000
d2 =		4.1000	4.1000	4.1000	4.1000	4.1000
IRF0 =		32.4000	39.0000	39.0000	39.0000	39.0000
irC =		0.0190	0.0190	0.0190	0.0190	0.0190
irT =		4.1650	4.1650	4.1650	4.1650	4.1650
fco22x =		4.2000	4.2000	4.2000	4.2000	4.2000

Appendix DFAIR-4

The equations of the DFAIR model as of February 2023 are the following. (FAIR-beta-4-3-1.gms)

```
** Equals old FAIR with recalibrated parameters for revised F2xco2 and Millar model.
** Deletes nonnegative reservoirs. See explanation below

sets    tfirst(t), tlast(t);

PARAMETERS
      yr0    Calendar year that corresponds to model year zero        /2020/
     emshare0 Carbon emissions share into Reservoir 0   /0.2173/
     emshare1 Carbon emissions share into Reservoir 1    /0.224/
     emshare2 Carbon emissions share into Reservoir 2    /0.2824/
     emshare3 Carbon emissions share into Reservoir 3    /0.2763/
     tau0    Decay time constant for R0  (year)                    /1000000/
     tau1    Decay time constant for R1  (year)                    /394.4/
     tau2    Decay time constant for R2  (year)      /36.53/
     tau3    Decay time constant for R3  (year) /4.304/

     teq1    Thermal equilibration parameter for box 1 (m^2 per KW)        /0.324/
     teq2    Thermal equilibration parameter for box 2 (m^2 per KW)       /0.44/
     d1     Thermal response timescale for deep ocean (year)            /236/
     d2     Thermal response timescale for upper ocean (year)           /4.07/

     irf0    Pre-industrial IRF100 (year)                          /32.4/
     irC     Increase in IRF100 with cumulative carbon uptake (years per GtC)    /0.019/
     irT     Increase in IRF100 with warming (years per degree K)            /4.165/
     fco22x   Forcings of equilibrium CO2 doubling (Wm-2)                   /3.93/

** INITIAL CONDITIONS TO BE CALIBRATED TO HISTORY
** CALIBRATION
     mat0   Initial concentration in atmosphere in 2020 (GtC)      /886.5128014/
     res00  Initial concentration in Reservoir 0 in 2020 (GtC)     /150.093 /
     res10  Initial concentration in Reservior 1 in 2020 (GtC)     /102.698 /
     res20  Initial concentration in Reservoir 2 in 2020 (GtC)     /39.534  /
     res30  Initial concentration in Reservoir 3 in 2020 (GtC)     / 6.1865 /
     mateq      Equilibrium concentration atmosphere  (GtC)         /588   /
     tbox10    Initial temperature box 1 change in 2020 (C from 1765)  /0.1477  /
     tbox20    Initial temperature box 2 change in 2020 (C from 1765)  /1.099454/
     tatm0     Initial atmospheric temperature change in 2020         /1.24715 /
   ;
VARIABLES
*Note: Stock variables correspond to levels at the END of the period
      FORC(t)       Increase in radiative forcing (watts per m2 from 1765)
      TATM(t)       Increase temperature of atmosphere (degrees C from 1765)
      TBOX1(t)      Increase temperature of box 1 (degrees C from 1765)
      TBOX2(t)      Increase temperature of box 2 (degrees C from 1765)
      RES0(t)       Carbon concentration in Reservoir 0 (GtC from 1765)
      RES1(t)       Carbon concentration in Reservoir 1 (GtC from 1765)
      RES2(t)       Carbon concentration in Reservoir 2 (GtC from 1765)
      RES3(t)       Carbon concentration in Reservoir 3 (GtC from 1765)
      MAT(t)        Carbon concentration increase in atmosphere (GtC from 1765)
      CACC(t)       Accumulated carbon in ocean and other sinks (GtC)
      IRFt(t)       IRF100 at time t
      alpha(t)      Carbon decay time scaling factor
      SumAlpha      Placeholder variable for objective function;
```

```
**** IMPORTANT PROGRAMMING NOTE. Earlier implementations has reservoirs as non-negative.
**** However, these are not physical but mathematical solutions.
**** So, they need to be unconstrained so that can have negative emissions.
NONNEGATIVE VARIABLES   TATM, MAT,  IRFt, alpha
EQUATIONS
      FORCE(t)       Radiative forcing equation
      RES0LOM(t)     Reservoir 0 law of motion
      RES1LOM(t)     Reservoir 1 law of motion
      RES2LOM(t)     Reservoir 2 law of motion
      RES3LOM(t)     Reservoir 3 law of motion
      MMAT(t)        Atmospheric concentration equation
      Cacceq(t)      Accumulated carbon in sinks equation
      TATMEQ(t)      Temperature-climate equation for atmosphere
      TBOX1EQ(t)     Temperature box 1 law of motion
      TBOX2EQ(t)     Temperature box 2 law of motion
      IRFeqLHS(t)    Left-hand side of IRF100 equation
      IRFeqRHS(t)    Right-hand side of IRF100 equation
;
** Equations of the model
   res0lom(t+1)..  RES0(t+1) =E=  (emshare0*tau0*alpha(t+1)*(Eco2(t+1)/3.667))*(1-exp(-
tstep/(tau0*alpha(t+1))))+Res0(t)*exp(-tstep/(tau0*alpha(t+1)));
   res1lom(t+1)..  RES1(t+1) =E=  (emshare1*tau1*alpha(t+1)*(Eco2(t+1)/3.667))*(1-exp(-
tstep/(tau1*alpha(t+1))))+Res1(t)*exp(-tstep/(tau1*alpha(t+1)));
   res2lom(t+1)..  RES2(t+1) =E=  (emshare2*tau2*alpha(t+1)*(Eco2(t+1)/3.667))*(1-exp(-
tstep/(tau2*alpha(t+1))))+Res2(t)*exp(-tstep/(tau2*alpha(t+1)));
   res3lom(t+1)..  RES3(t+1) =E=  (emshare3*tau3*alpha(t+1)*(Eco2(t+1)/3.667))*(1-exp(-
tstep/(tau3*alpha(t+1))))+Res3(t)*exp(-tstep/(tau3*alpha(t+1)));
   mmat(t+1)..     MAT(t+1)  =E=   mateq+Res0(t+1)+Res1(t+1)+Res2(t+1)+Res3(t+1);
   cacceq(t)..     Cacc(t)   =E=  (CCATOT(t)-(MAT(t)-mateq));
   force(t)..      FORC(t)   =E=  fco22x*((log((MAT(t)/mateq))/log(2))) + F_Misc(t)+F_GHGabate(t);

   tbox1eq(t+1)..  Tbox1(t+1) =E=  Tbox1(t)*exp(-tstep/d1)+teq1*Forc(t+1)*(1-exp(-tstep/d1));
   tbox2eq(t+1)..  Tbox2(t+1) =E=  Tbox2(t)*exp(-tstep/d2)+teq2*Forc(t+1)*(1-exp(-tstep/d2));
   tatmeq(t+1)..   TATM(t+1)  =E=   Tbox1(t+1)+Tbox2(t+1);
   irfeqlhs(t)..   IRFt(t)   =E=  ((alpha(t)*emshare0*tau0*(1-exp(-100/(alpha(t)*tau0))))+(alpha(t)*emshare1*tau1*(1-exp(-
100/(alpha(t)*tau1))))+(alpha(t)*emshare2*tau2*(1-exp(-100/(alpha(t)*tau2))))+(alpha(t)*emshare3*tau3*(1-exp(-
100/(alpha(t)*tau3)))));
   irfeqrhs(t)..   IRFt(t)   =E=  irf0+irC*Cacc(t)+irT*TATM(t);
**  Upper and lower bounds for stability
MAT.LO(t)      = 10;
TATM.UP(t)     = 20;
TATM.lo(t)     = .5;
alpha.up(t) = 100;
alpha.lo(t) = 0.1;
* Initial conditions
MAT.FX(tfirst)    = mat0;
TATM.FX(tfirst)   = tatm0;
Res0.fx(tfirst) = Res00;
Res1.fx(tfirst) = Res10;
Res2.fx(tfirst) = Res20;
Res3.fx(tfirst) = Res30;
Tbox1.fx(tfirst) = Tbox10;
Tbox2.fx(tfirst) = Tbox20;
** Solution options
option iterlim = 99900;
option reslim = 99999;
option solprint = on;
option limrow = 0;
option limcol = 0;
```

Background Note on Non-CO2 Forcings
October 26, 2023

Advice on Background Notes on Non-CO2 Forcings: These background notes are for informational purposes for modelers. They are not intended for publication and are not publication quality. Some of the details are sketched and not derived in detail in this document. They may be cited with the warning, "Background notes are for informational purposes and are not published."

I. Overview

The treatment of land emissions and non-CO2 greenhouse gases is changed in the current DICE model. In earlier treatments, land emissions and non-CO2 GHGs were exogenous. In the current treatment, land emissions are endogenous and included with industrial CO2, while non-CO2 GHG emissions are divided into abatable and non-abatable. The abatable non CO2 greenhouse gases are included as a CO2 equivalent. Because the stock-flow-forcings relationship for non-CO2 emissions is simplified, there are small discrepancies in the results relative to complete earth-systems models.

II. Emissions data and projections

Land CO2 emissions were excluded from abatable emissions in earlier versions. Additionally, a major problem with the earlier treatment was that it assumed that land emissions decline sharply over time. If we look at IPCC estimates, we see a 0.7% per year increase in land per year over last forty years. This changes the outlook considerably for non-industrial CO2. In the new simulations, the baseline land emissions are changed to minus 2% per year.

	1750–2019 Cumulative (PgC)	1850-2019 Cumulative (PgC)	1980–1989 Mean Annual Growth Rate (PgC yr^{-1})	1990–1999 Mean Annual Growth Rate (PgC yr^{-1})	2000–2009 Mean Annual Growth Rate (PgC yr^{-1})	2010–2019 Mean Annual Growth Rate (PgC yr^{-1})
Emissions						
Fossil fuel combustion and cement production	445 ± 20	445 ± 20	5.4 ± 0.3	6.3 ± 0.3	7.7 ± 0.4	9.4 ± 0.5
Net land use change	240 ± 70	210 ± 60	1.3 ± 0.7	1.4 ± 0.7	1.4 ± 0.7	1.6 ± 0.7
Total emissions	685 ± 75	655 ± 65	6.7 ± 0.8	7.7 ± 0.8	9.1 ± 0.8	10.9 ± 0.9
Partition						
Atmospheric increase	285 ± 5	265 ± 5	3.4 ± 0.02	3.2 ± 0.02	4.1 ± 0.02	5.1 ± 0.02
Ocean sink[c]	170 ± 20	160 ± 20	1.7 ± 0.4	2.0 ± 0.5	2.1 ± 0.5	2.5 ± 0.6
Terrestrial sink	230 ± 60	210 ± 55	2.0 ± 0.7	2.6 ± 0.7	2.9 ± 0.8	3.4 ± 0.9
Budget imbalance	0	20	–0.4	–0.1	0	–0.1

Table Note-NC-1. IPCC AR6 Calculations on Emissions (Table 5.1), with label as follows:

Global anthropogenic CO_2 budget accumulated since the industrial revolution (onset in 1750) and averaged over the 1980s, 1990s, 2000s, and 2010s. By convention, a negative ocean or land to atmosphere CO_2 flux is equivalent to a gain of carbon by these reservoirs. The table does not include natural exchanges (e.g. rivers, weathering) between reservoirs. Uncertainties represent the 68% confidence interval (Friedlingstein et al., 2020).

Next, if we look at historical emissions of CO2 and CO2-2, we see that CO2-e has grown a little more slowly than fossil CO2 over period 1970 – 2018 (0.2% per year more slowly).

	Average annual growth rate		
Period	CO2-e	CO2	Difference
1970-2021	1.5%	1.7%	-0.19%
2000-2021	1.6%	1.8%	-0.20%
Source: non-c02vco2 history-010323.xls			

Table Note-NC-2. Historical growth CO2 and CO2-e emissions.

Item	2020	2025	2050	2100
Base/NC industrial emissions (GtCO2/yr)	39.55	43.38	61.12	78.54
Base/NC land emissions (GtCO2/yr)	5.90	5.31	3.14	1.09
Abateable nonCO2 emissions GHG (GtCO2e/yr)	9.24	9.56	11.14	14.30
Total, CO2-e abateable emissions (GtCO2e/yr)	**54.69**	**58.24**	**75.39**	**93.93**
Base/NC CO2 forcings (W/m2)	2.43	2.69	4.04	6.62
Abateable other forcings (w/m2)	1.16	1.10	1.04	1.28
Exogenous forcings (w/m2)	(0.20)	(0.16)	0.04	0.44
Total abateable forcings (w/m2)	**3.39**	**3.63**	**5.12**	**8.34**

Base/NC = with zero emissions control

Source: non-co2GHG-MAC-up010323.xls

Table Note-NC-3. Projections CO2 and CO2-e emissions.

Item	Growth, 2020-2100
Base/NC industrial emissions (GtCO2/yr)	0.86%
Base/NC land emissions (GtCO2/yr)	-2.09%
Abateable nonCO2 emissions GHG (GtCO2e/yr)	0.55%
Total, CO2-e abateable emissions (GtCO2e/yr)	0.68%
Base/NC CO2 forcings (W/m2)	1.26%
Abateable other forcings (w/m2)	0.12%
Exogenous forcings (w/m2)	na
Total abateable forcings (w/m2)	1.13%

Base/NC = with zero emissions control

Source: non-co2GHG-MAC-up010323.xls

Table Note-NC-4. Projections of growth of CO2 and CO2-e emissions.

III. Abatement costs

The abatement cost function is drawn from Harmsen 2019. The maximum reduction at the CO2 backstop of $480 is 57% in 2050; and about 69% in 2100. The curve is more convex that for CO2. However, this may be because it is constructed using engineering approaches. We assume that the mitigation cost function is the same and that the abatable part is 65% of non-CO2-GHG.

The following shows the marginal cost function for CO2 and non-CO2 GHGs from DICE and Harmsen. Note that the price/marginal cost curve for non-CO2 GHG's is much more convex than for CO2.

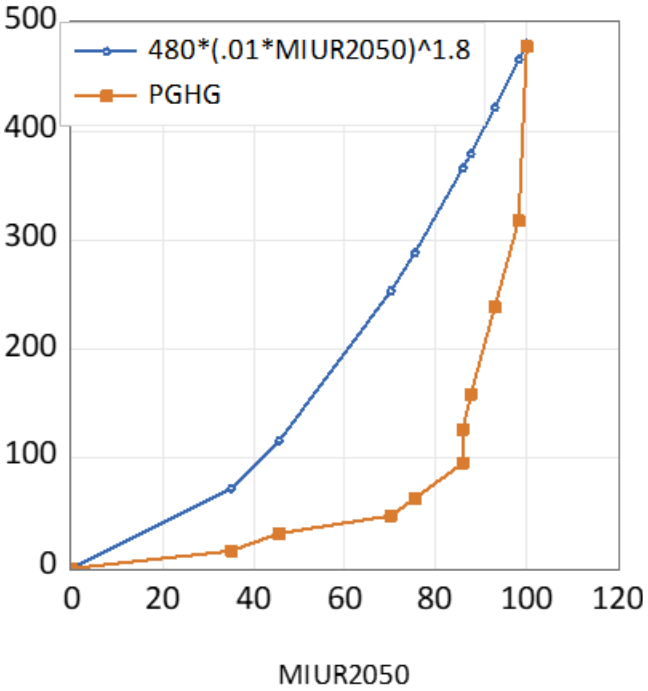

Figure Note-NC-1. Projections of growth of CO2 and CO2-e emissions.

[Source; Lab Notes for DICE.]

The following is the regression of the marginal cost on the emissions control rate for the Harmsen data, showing the higher convexity.

Dependent Variable: LOG(PGHG)
Method: Least Squares
Date: 12/20/21 Time: 14:00
Sample: 2 11
Included observations: 10

Variable	Coefficient	Std. Error	t-Statistic	Prob.
C	-7.442956	1.881006	-3.956901	0.0042
LOG(MIUR2050)	2.800396	0.435560	6.429421	0.0002

R-squared	0.837851	Mean dependent var	4.615397
Adjusted R-squared	0.817583	S.D. dependent var	1.065225
S.E. of regression	0.454961	Akaike info criterion	1.439648
Sum squared resid	1.655918	Schwarz criterion	1.500165
Log likelihood	-5.198238	Hannan-Quinn criter.	1.373261
F-statistic	41.33745	Durbin-Watson stat	0.581986
Prob(F-statistic)	0.000203		

Table Note-NC-5. Projections of growth of CO2 and CO2-e emissions.

[Source; Lab Notes for DICE.]

IV. Forcings and carbon price error

The issue with the non-CO2 gases is that they cannot easily be translated from forcings into CO2e and the reverse. I had originally thought that we could multiple CO2 by a forcings ratio to get CO2e. However, this is inaccurate. The reason is that dF/dCO2 differs with the level of concentrations. A little experimentation also shows that it is not obvious how to put in a correction factor. The calculation of dF/dCO2 is not the natural = constant/M(t) (from logarithmic derivative).

Additionally, the treatment leads to error in calculation of the carbon price and SCC. Some experimentation showed that this was because of the addition of GHGs other than industrial CO2. See the following table:

Ratio SCC/cprice							
Year	2020	2025	2030	2035	2040	2045	2050
NO NON-CO2 GHG	1.19	0.89	0.91	0.92	0.93	0.94	0.95
ALL GHG	1.33	1.03	1.04	1.05	1.06	1.06	1.05
ONLY IND CO2	1.16	1.00	1.00	1.00	1.00	1.00	1.00
NO NON-CO2 GHG	19.4%	-10.9%	-9.2%	-7.8%	-6.6%	-5.6%	-4.9%
ALL GHG	33.2%	3.3%	4.5%	5.2%	5.6%	5.6%	5.4%
ONLY IND CO2	16.3%	0.0%	0.0%	0.0%	0.0%	0.0%	0.0%

Table Note-NC-6. Error in carbon price due to non-CO2 GHGs.

[Source; Lab Notes for DICE.]

V. GAMS model for non-CO2 GHGs

The following is the GAMS code for non-CO2 GHGs, "Nonco2-b-4-3-1.gms". Note that this is an "Include" subroutine.

```
 ==================

* nonco2 Parameters
Parameters
     CO2E_GHGabateB(t)       Abateable non-CO2 GHG emissions base
     CO2E_GHGabateact(t)     Abateable non-CO2 GHG emissions base (actual)
     F_Misc(t)               Non-abateable forcings (GHG and other)
     emissrat(t)             Ratio of CO2e to industrial emissions
     sigmatot(t)             Emissions output ratio for CO2e
     FORC_CO2(t)             CO2 Forcings
;
** Parameters for non-industrial emission
** Assumes abateable share of non-CO2 GHG is 65%
Parameters
     eland0       Carbon emissions from land 2015 (GtCO2 per year)  / 5.9    /
     deland       Decline rate of land emissions (per period)      / .1     /
     F_Misc2020   Non-abatable forcings 2020                    /  -0.054    /
     F_Misc2100   Non-abatable forcings 2100                     / .265/
     F_GHGabate2020 Forcings of abatable nonCO2 GHG               / 0.518 /
     F_GHGabate2100 Forcings of abatable nonCO2 GHG               / 0.957 /
     ECO2eGHGB2020  Emis of abatable nonCO2 GHG GtCO2e  2020          /  9.96/
     ECO2eGHGB2100  Emis of abatable nonCO2 GHG GtCO2e  2100          /  15.5 /
     emissrat2020   Ratio of CO2e to industrial CO2 2020             / 1.40 /
     emissrat2100   Ratio of CO2e to industrial CO2 2020             / 1.21 /
     Fcoef1       Coefficient of nonco2 abateable emissions         /0.00955/
     Fcoef2       Coefficient of nonco2 abateable emissions         /.861/
     ;
** Parameters emissions and non-CO2
     eland(t) = eland0*(1-deland)**(t.val-1); eland(t) = eland0*(1-deland)**(t.val-1);
     CO2E_GHGabateB(t)=ECO2eGHGB2020+((ECO2eGHGB2100-ECO2eGHGB2020)/16)*(t.val-1)$(t.val le
16)+((ECO2eGHGB2100-ECO2eGHGB2020))$(t.val ge 17);
     F_Misc(t)=F_Misc2020 +((F_Misc2100-F_Misc2020)/16)*(t.val-1)$(t.val le 16)+((F_Misc2100-
F_Misc2020))$(t.val ge 17);
     emissrat(t) = emissrat2020 +((emissrat2100-emissrat2020)/16)*(t.val-1)$(t.val le 16)+((emissrat2100-
emissrat2020))$(t.val ge 17);
     sigmatot(t) = sigma(t)*emissrat(t);
     cost1tot(t) = pbacktime(T)*sigmatot(T)/expcost2/1000;
VARIABLES
     ECO2(t)       Total CO2 emissions (GtCO2 per year)
     ECO2E(t)      Total CO2e emissions including abateable nonCO2 GHG (GtCO2 per year)
     EIND(t)       Industrial CO2 emissions (GtCO2 per yr)
     F_GHGabate    Forcings abateable nonCO2 GHG
;
Equations
     ECO2eq(t)       CO2 Emissions equation
     ECO2Eeq(t)      CO2E Emissions equation
     EINDeq(t)       Industrial CO2 equation
     F_GHGabateEQ(t);
```

These endnotes provide the sources for figures and tables.

[i] Source: test-dist-092923.wf1; sdf-exp-v10-npp-02.prg. Tabulated in Results-MOnte-Carlo-090523-u092923a.xlsx.

[ii] Source: figure1_draws-avggrowth.xls.

[iii] Also see Copy of GIVE_discount_rate_decomposition; Results-MOnte-Carlo-090523;

[iv] Source: Capital rates of returns 070623, page "wn-ror-nipa"

[v] Source: gdp-compar-100423.xlsx

[vi] Source: gdp-compar-100423.xlsx

[vii] Source: figure is "fig_forecast_growth" in from program long-term- g-reg-092923.prg and data ghghistory-081223.wf1.